Atmos. Meas. Tech., 18, 2373–2396, 2025
https://doi.org/10.5194/amt-18-2373-2025

Atmospheric Measurement Techniques
Open Access
EGU

CIAO main upgrade: building up an ACTRIS-compliant aerosol in situ laboratory

Teresa Laurita, Alessandro Mauceri, Francesco Cardellicchio, Emilio Lapenna, Benedetto De Rosa, Serena Trippetta, Michail Mytilinaios, Davide Amodio, Aldo Giunta, Ermann Ripepi, Canio Colangelo, Nikolaos Papagiannopoulos, Francesca Morrongiello, Claudio Dema, Simone Gagliardi, Carmela Cornacchia, Rosa Maria Petracca Altieri, Aldo Amodeo, Marco Rosoldi, Donato Summa, Gelsomina Pappalardo, and Lucia Mona

Consiglio Nazionale delle Ricerche – Istituto di Metodologie per l'Analisi Ambientale CNR-IMAA, C. da S. Loja, Tito Scalo, Potenza, 85050, Italy

Correspondence: Teresa Laurita (teresa.laurita@cnr.it)

Received: 27 March 2024 – Discussion started: 13 May 2024
Revised: 30 November 2024 – Accepted: 2 March 2025 – Published: 4 June 2025

Abstract. This paper describes the aerosol in situ laboratory at the CNR-IMAA (Consiglio Nazionale delle Ricerche – Istituto di Metodologie per l'Analisi Ambientale) Atmospheric Observatory (CIAO) in southern Italy, outlining its configuration and detailing each instrument and sampling line. CIAO has been collecting observations of atmospheric components since 2000. Initially, the activities revolved around aerosol lidar; radiosounding and cloud remote sensing observations were added over the years and made CIAO a leading atmospheric observatory in the Mediterranean region. In 2018, a significant upgrade was started to enhance the observational capability of the observatory by adding aerosol in situ instruments, with the objective to push new research boundaries for aerosol particle characterization and multi-instrument combined approaches. Here, we describe each technical implementation step for building up an extensive aerosol in situ laboratory compliant with ACTRIS (Aerosol, Clouds and Trace gases Research Infrastructure) standard operating procedures. Starting from scratch, the long path was initiated in 2018 with the design of the laboratory in terms of instruments, container layout, inlets, and sampling lines, as well as required time and interactions with experts in the field. Reporting on all the details regarding the final solutions implemented at CIAO, this paper will be, for new aerosol in situ laboratories, a practical guide for the implementation of the aerosol in situ observational site.

1 Introduction

The importance of a quantitative and qualitative assessment of atmospheric aerosol particle characteristics has been recognized for many years: aerosol particles are responsible for direct and indirect effects on atmospheric processes, affecting climate and human health, as well as the precipitation cycle and air quality (e.g. Pöschl, 2005; Ren-Jian et al., 2012; IPCC, 2021). Depending on their sources, aerosol particles appear in different sizes and/or shapes, and their relatively short lifetime makes the physical and chemical properties extremely variable on both temporal and spatial scales. Because of the inherent complexity of aerosol particles, a single measurement technique providing all the relevant information is not available: thus, a multi-instrument approach is needed. The combination of different techniques and observational platforms can be crucial for a better understanding of the presence and the characteristics of atmospheric aerosol particles, as well as their role in the large variety of processes in which they are involved. The Aerosol, Clouds and Trace gases Research Infrastructure (ACTRIS, 2023; Laj et al., 2024) is the European research infrastructure (RI) aiming to integrate previous existing networks for the characterization of aerosol particles, clouds, and trace gases using and integrating in situ and remote sensing observations and experimental platforms for the characterization of atmospheric components under controlled environments. An overarching investigation of the atmosphere which accounts for all three of these components is a winning strategy: for instance, aerosol particles act as cloud condensation nuclei

(CNN) affecting the cloud properties and lifetime; emitted gas species may act as precursors to form new particles in the atmosphere, i.e. the secondary aerosol particle. Integrated approaches of remote sensing and in situ observations allow us to take the most from the detailed and accurate characterization in terms of the morphology of particles, dimension, and chemical composition: the remote sensing provides the vertical profile of physical and optical property information, which is essential for investigating aerosol layers, long-range transportation, mixing processes, and aerosol–cloud interactions; the latter is the only approach to provide the chemical composition and reliable data at ground level, where aerosol particles affect ecosystems and humans.

In this scenario, the CNR-IMAA Atmospheric Observatory (CIAO; Madonna et al., 2011), operating since 2000, has recently been upgraded with the aerosol in situ observational component, thus complementing the multi-year high-quality aerosol remote sensing data record. The combination of the aerosol in situ measurements with remote sensing observations is expected to strengthen fundamental knowledge about aerosol particle impacts on human health, ecosystems, and climate. This combination can be achieved by either comparing or complementing the techniques: the results of the comparison will allow us to reduce the uncertainty of aerosol particle measurements in the atmosphere, with a subsequent improvement in model predictions regarding climate change, whereas the complementarity results in the possibility of investigating the aerosol particles from the ground up to the stratosphere. The new aerosol in situ facility at CIAO, funded by the Italian Ministry of University and Research through the PER-ACTRIS-IT project (2023), has received initial acceptance as an ACTRIS National Facility observational platform for the measurements of, at least, the obligatory ACTRIS aerosol in situ variables. The site begun the next phase of the labelling process in 2024, a key element of ACTRIS's data quality assurance system. This process ensures that instruments, data, and methodologies used across ACTRIS observational platforms meet specific quality criteria. The labelling process involves a series of evaluations and certifications to verify compliance with ACTRIS protocols (Deliverable 5.1, 2024). During the labelling process, the National Facilities are annually invited by CAIS-ECAC (Center for Aerosol In Situ – European Centre for Aerosol Calibration and Characterization) to calibration workshops, where instruments are calibrated and where the quality of the data is thoroughly verified.

In this paper, we present a concise overview of the observatory, focusing on the characteristics of the recently established ACTRIS-compliant in situ facility, with the main aim being to benefit the aerosol community by providing a comprehensive and detailed description of technical solutions for the implementation of such a component. Being a guide for the building up of an ACTRIS aerosol in situ station, it is potentially also of interest also for extra-European communities or communities outside of ACTRIS: the ACTRIS in situ standards are, in some way, following those of the WMO/GAW (World Meteorological Organization/-Global Atmosphere Watch; WMO/GAW, 2016); therefore, the interest in technical solutions for an ACTRIS-compliant in situ instrumentation is shown by more than just the stations potentially involved in ACTRIS. Additionally, new EU air quality directives will include some more advanced stations where black carbon and ultrafine measurements should be collected. Therefore, solutions adopted for collecting such measurements with ACTRIS standards could be of interest for air quality management networks in order to guarantee the quality of the collected data.

After a short description of CIAO and its typical atmospheric conditions in Sect. 2, Sect. 3 reports on the remote sensing instrumentation currently operating at CIAO. Section 4 represents the core of this paper, providing the in-depth description of the in situ facility, with the detailed configuration of each instrument and sampling line. Finally, Sect. 5 illustrates three scientific topics to be studied at CIAO with the combined deployment of aerosol in situ and remote sensing measurements.

2 Description of the site

Equipped with state-of-the-art systems for remote sensing and in situ measurements of aerosol particles, CIAO (2023) is currently a reference station for short-lived atmospheric constituents in Italy and the Mediterranean. The site is located in the southern Apennines in Italy (Tito Scalo; 40.60° N, 15.72° E; 760 m a.s.l.), in a plain surrounded by low mountains, less than 150 km away from the western, southern, and eastern coasts (Fig. 1).

Therefore, it operates in typical mountainous weather strongly influenced by Mediterranean atmospheric circulation, resulting in generally dry, hot summers and cold winters. Indeed, between 2004 and 2017, dew point temperatures at the station after sunset exceeded 15 °C during summer only (Fig. 2). The prevailing wind direction occurring at the site is W–WSW–SW (Fig. 3).

Most of the surrounding land is classified as arable crops in non-irrigated areas, followed by broad-leaved woods and coniferous forests, sclerophyllous or wooded or shrubby areas, and natural-grazing areas and grasslands (Regione Basilicata, 2023).

CIAO's mission is to improve the knowledge of atmospheric processes and their role in meteorological phenomena, climate change, and air quality. Given the coverage and global relevance of the processes studied, fundamental aspects of the activities and approaches adopted are the development of internationally recognized Standard Operating Procedures, the open-data policy, and the full sharing of methodologies and know-how.

CIAO provides free and open-access data to national and international users like researchers, small- and medium-

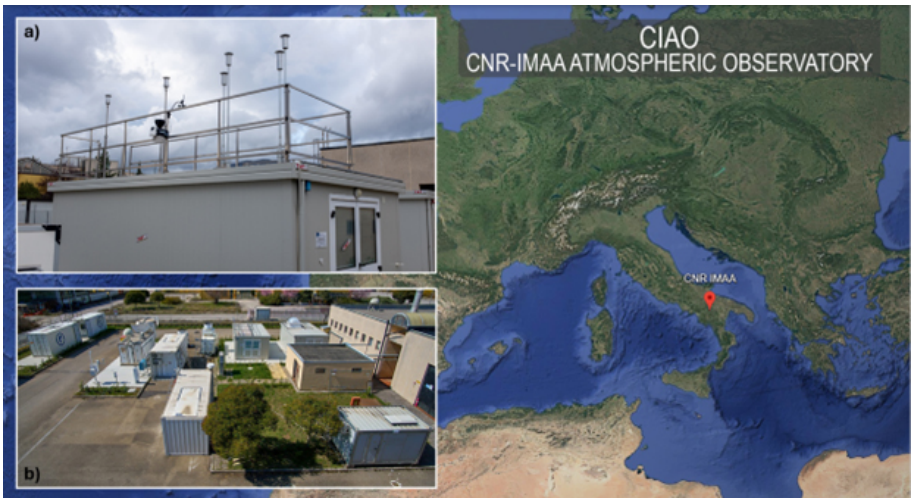

Figure 1. Location of the CNR-IMAA Atmospheric Observatory (© Google Earth); **(a)** overview of the aerosol in situ facility and **(b)** overview of all CIAO infrastructures.

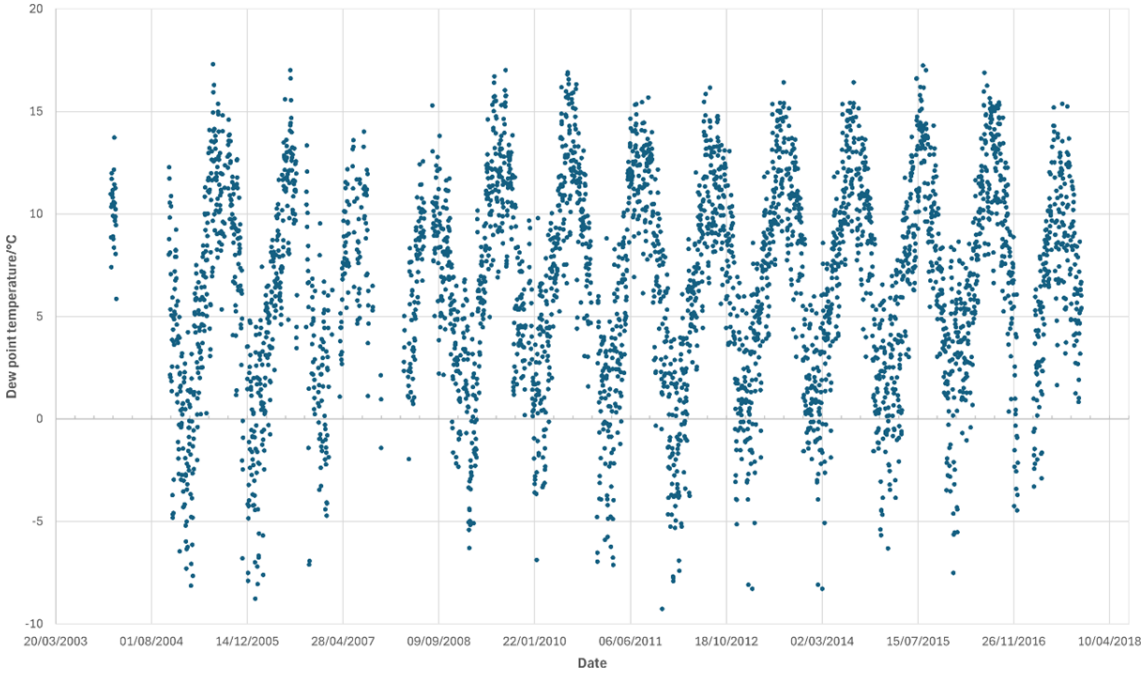

Figure 2. Dew point temperature time series at CIAO in the time frame of 2004–2017, obtained from continuous measurements of the automatic weather station VAISALA MILOS520, with daily means.

sized enterprises (SMEs), students, and citizens. At the present time, CIAO extends its outreach through the ATMO-ACCESS Trans-National Access programme (2023). This programme allows participants to engage in research on aerosol particles and their effects, to learn techniques and methods, to contribute instruments, or to collaborate with the team.

The research activities of CIAO evolved around the long-term observations of aerosol particles, clouds, trace gases, and greenhouse gases within the European research infrastructures ACTRIS and ICOS (Integrated Carbon Observing System), as well as around the participation of CIAO in reference observational programmes and networks on a global scale, such as GRUAN (GCOS (Global Climate Observing System) Reference Upper-Air Network) and GALION (GAW Aerosol Lidar Observation Network). The observational strategy is organized to provide quality-assured data for satellite validation and model evaluation and to fully exploit the synergy and integration of the active and passive sensors for the improvement of the atmospheric characteriza-

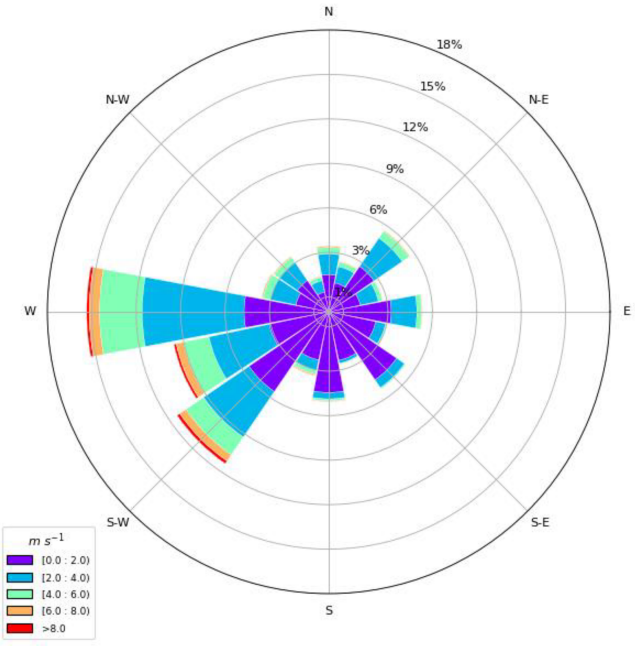

Figure 3. Wind rose diagram at CIAO in 2004–2017 obtained from continuous measurements of the automatic weather station VAISALA MILOS520, with a temporal resolution of 1 min.

tion (e.g. Pappalardo et al., 2004b; Mona et al., 2009; Boselli et al., 2012; Ilić et al., 2022). The complete list of CIAO publications is available at https://ciao.imaa.cnr.it/publications/ (last access: 10 December 2023).

With regard to the types of aerosol particles measured, CIAO, due to its geographical position and low background concentration of aerosol particles, is particularly well suited for studying naturally occurring particles such as desert dust and volcanic ash clouds. The site is regularly affected by Saharan dust intrusions (e.g. Mona et al., 2006, 2014; Binietoglou et al., 2015; Soupiona et al., 2020) and was reached by volcanic aerosol particles at the level of the free troposphere during the eruptions of the Etna (e.g. Pappalardo et al., 2004a; Villani et al., 2006) and Eyjafjallajökull (Madonna et al., 2010; Mona et al., 2012; Pappalardo et al., 2013) volcanos in 2002 and 2010, respectively, in addition to being reached by volcanic aerosol particles in the stratospheric layers (e.g. Sawamura et al., 2012). In recent years, the observatory has become actively involved in the study of smoke plumes originating from wildfires, occurring as both short-range-transported plumes, spreading with increased frequency in the surrounding forestry areas during the summer period (De Rosa et al., 2022), and long-range-transported plumes, such as the autumn 2020 California wildfires, whose smoke, transported in the stratosphere, reached the site within 13 d (Baars et al., 2019).

3 Remote sensing measurements

Remote sensing measurements have been the backbone of the research activity at CIAO since its beginning in the early 2000s, with the scientific goal of providing long-term measurements for the climatology of aerosol and cloud properties.

Besides the compliance with the ACTRIS guidelines, all the remote sensing measurements performed at CIAO are designed to be in line with the main ground-based observation networks (i.e. EARLINET (European Aerosol Research Lidar Network to Establish an Aerosol Climatology), CloudNet, AERONET (Aerosol Robotic Network), GRUAN, GALION) and the major international standards provided by the WMO/GAW 2016, aiming to establish a long-term, harmonized, and statistically significant database of measurements of atmospheric parameters and constituents for climatological studies (Matthias et al., 2004).

The active remote sensing instruments operative at CIAO include multi-wavelength Raman and polarization lidars, ceilometers, Doppler lidars, and polarimetric Doppler radars, and the passive ones include microwave radiometers, photometers, and a high-resolution Fourier-transform infrared (FTIR) spectrometer.

With respect to the status of CIAO as reported in previous papers (e.g. Madonna et al., 2011), some instruments are still operating, some have been replaced by more recent and advanced ones, and new instruments for increasing the observational capabilities have been added.

For the aerosol remote sensing, two new highly advanced lidar systems have been recently installed at CIAO, one fixed and one mobile. They are able to provide measurements of the vertical profiles of several aerosol optical properties, namely backscatter coefficient and particle depolarization at 1064, 532, and 355 nm and extinction coefficient at 532 and 355 nm, with the observational range starting from 200 m and extending up to at least 20 km of altitude. The two systems are reference lidars for ACTRIS and also offer services to test the performances of other lidar systems through on-site direct intercomparison campaigns using the mobile lidar.

Closely related to the aerosol multi-wavelength depolarization Raman, a triple-mode photometer is operational within AERONET and ACTRIS, providing columnar aerosol optical depth measurements and columnar size distribution information, not only during the daytime but also during the nighttime under certain illumination conditions. CIAO is also equipped with a lidar laboratory and an optical laboratory, which allow us to implement and test several customized lidar configurations and to test and characterize optical components and laser sources typically used in high-power lidar systems.

Besides the aerosol remote sensing instruments, the cloud remote sensing equipment has also been updated and expanded with additional complementary instruments, and a high-resolution FTIR spectrometer has been added for per-

forming remote sensing measurements of trace gases to complement the other observations.

The availability of a large number of remote sensing systems at the observatory has enabled the possibility to both compare and combine different techniques for studying atmospheric parameters (e.g. Mona et al., 2007; Madonna et al., 2010; Boselli et al., 2012; Lopatin et al. 2013; Madonna et al., 2015).

A synergistic approach has been proposed for the study of thin liquid-water clouds, combining multi-wavelength lidar and Doppler radar measurements (Rosoldi et al., 2022). It has been shown that a microwave radiometer can be used to calibrate Raman lidar measurements for water vapour profiling and that the synergy between these instruments is an effective means for atmospheric water vapour monitoring (Madonna et al., 2006, Mona et al., 2007).

However, despite its huge potential in atmospheric research, there are two major drawbacks associated with the remote sensing observations: the inability to conduct aerosol measurements under skies with low clouds and precipitations, along with the impossibility of characterizing the particulate properties near the ground. Therefore, the recent implementation of the in situ facility described in the next section is fundamental to achieve a complete characterization of the aerosol at the ground level, where the aerosol particles directly affect ecosystems and human health. In addition, the in situ measurements include the valuable chemical characterization of the particulate matter (PM), thus providing a deeper comprehension of the aerosol type, the source apportionment, and the mixing atmospheric processes.

4 Description of the aerosol in situ facility

4.1 Overview

The in situ facility recently installed at CIAO comprises two main parts (Fig. 4): a field laboratory for aerosol particle online measurements, with continuous instrumentation and PM samplers, and a chemical laboratory for the post-sampling analysis of aerosol particles collected on filters. This facility enables the measurement of all obligatory ACTRIS aerosol in situ variables: particle number concentration of > 10 nm, particle number size distribution in terms of mobility diameter of 10 to 800 nm, particle light-scattering and backscattering coefficient, and particle light absorption coefficient and the equivalent black carbon concentration. Additionally, it allows the measurement of another four recommended variables: particle number size distribution in terms of aerodynamic diameter of 0.8 to 10 µm, mass concentration of particulate organic and elemental carbon, mass concentration of non-refractory particulate organics and inorganics, and mass concentration of particulate elements.

The shelter has been designed according to the ACTRIS guidelines and recommendations (Wiedensohler et al., 2014), with the instrumentation arranged as follows: a dual-spot aethalometer (AE33, Magee Scientific), a multi-wavelength integrating nephelometer (AURORA 3000, Ecotech), and an aerodynamic particle sizer (APS 3321, TSI) located downstream of a common PM_{10} (aerosol particles with an aerodynamic diameter of less than 10 µm) inlet and a time-of-flight aerosol chemical speciation monitor (ToF-ACSM, Aerodyne Research), a scanning mobility particle sizer (SMPS3938, TSI), and a condensation particle counter (CPC3750, TSI) placed downstream of a $PM_{2.5}$ (aerosol particles with an aerodynamic diameter of less 2.5 µm) common inlet. Additionally, two PM_x samplers (SWAM 5a Dual Channel Monitors, FAI Instruments) are installed at their respective inlets: one equipped with two $PM_{2.5}$ inlets and the other equipped with one PM_{10} inlet and one PM_1 inlet. Furthermore, a PM_x monitor (EDM 180, Grimm) is placed as a standalone instrument with an individual PM_{10} inlet line. Particular attention has been devoted to the design of the common inlets and the sampling lines. The PM_{10} and $PM_{2.5}$ common-impactor-type inlets, operating at a flow rate of $16.7\,\mathrm{L\,min^{-1}}$, are compliant with EN 12341 and EN 14907 standards, respectively. The main challenge when transporting aerosol particles to collectors and aerosol-particle-measuring instrumentation is to avoid particle losses. Therefore, firstly, the internal diameter of the main sampling pipe of the common PM_{10} and $PM_{2.5}$ inlets must be such that the sampled air has a laminar flow along the entire path (Reynolds number of less than 2000) to minimize the loss of particles by diffusion and inertia. The instrument sub-lines (characterized by smaller inside diameters) are connected to the two common PM_{10} and $PM_{2.5}$ inlets through their respective isokinetic flow splitters (Fig. 5), where the sample flow velocity closely matches the velocity of the main flow. Moreover, the tube ends in the isokinetic flow splitters must be sharp in order to minimize turbulence and to promote smooth airflow, ensuring uniform sampling. This design helps maintain laminar flow, reduces aerosol losses, and enhances the accuracy and reliability of measurements. Another key feature of the splitter is that the sample is collected from the core of the main aerosol flow rather than from streamlines near the wall of the main pipe, therefore ensuring a representative sampling (especially for coarse and nanoparticles).

The technical details of the common inlets and isokinetic splitters are shown in Table 1.

All the sampling tubes are kept as short as possible and are placed in a vertical position, with bends and connectors avoided as much as possible to suppress potential sources of turbulence, which would result in additional losses of particles. In addition, in accordance with ACTRIS recommendations, the tubes used are black sampling tubes supplied by the TSI company (2024). These TSI sampling tubes are made of conductive silicone, infused with black carbon to improve conductivity. This design is essential to minimize electrostatic losses, which can occur in non-conductive tubes, such as those made of standard silicone or Teflon, where particles

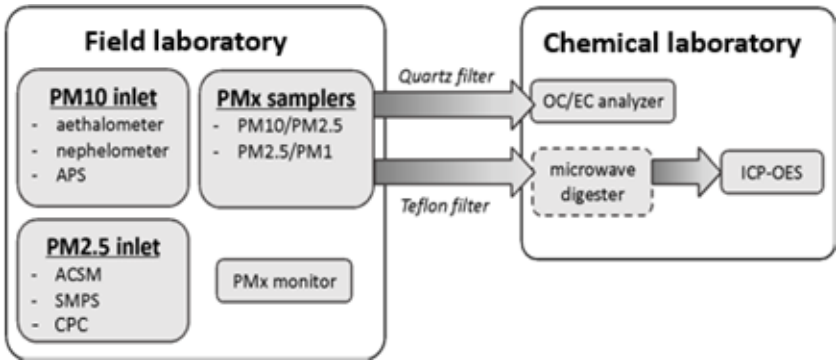

Figure 4. Outline of the workflow of the aerosol in situ facility at CIAO.

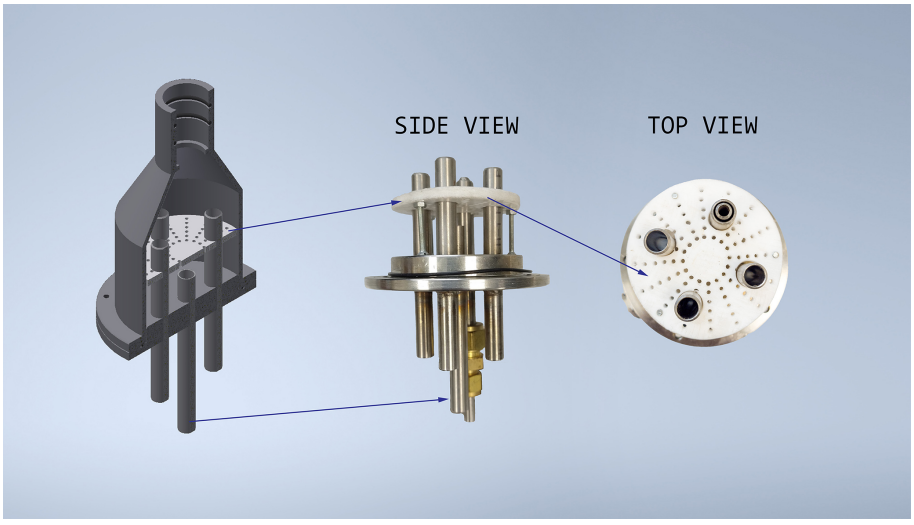

Figure 5. Image showing the rendering 3D of the isokinetic splitters, including the side view and top view (Quattro Esse, 2024).

can adhere to the tube walls due to static charges. The conductive nature of TSI tubes prevents the buildup of electrostatic fields, thus improving particle penetration and reducing sampling distortions caused by particle loss. The inlets on the rooftop of the field laboratory are placed 1 m away from each other and at heights of 1.5–2.0 m above the roof, corresponding to approximately 4.5–5 m above ground level, with the aim of minimizing local influences and potential interferences in the sampling process.

In compliance with the ACTRIS indications, all the instruments in the laboratory are equipped with a Nafion dryer tube, a specialized device made from a sulfonated tetrafluoroethylene-based polymer. This device is used in aerosol sampling to remove water vapour from the gas stream while preserving the chemical integrity of aerosol particles (Perma Pure, 2024). These Nafion dryers maintain the relative humidity (RH) to be well below 40 %; under this threshold, in fact, changes in particle diameter due to RH variations are expected to be lower than 5 %, thus obtaining comparable data independently of the hygroscopic behaviour of the aerosol particles. Moreover, the upstream drying prevents the possible instrument damage caused by water condensation.

The Nafion dryers of the aethalometer, nephelometer, APS, and ACSM operate in a reflux mode, as shown in Fig. 6, which returns the dry sample back to the dryer for use as the purge after it has gone through the analyser. Since this method uses all of the dry sample as purge air, only the sample flow required for analysis passes through the dryer. This results in a high drying efficiency. The vacuum on the purge air should be at least 15 in. Hg, with a higher vacuum preferable. This vacuum level is required to provide the desired 2 : 1 purge-to-sample flow ratio based on the actual volumetric flow. The 2 : 1 ratio ensures enough dry purge gas to continuously absorb moisture, preventing saturation and preserving sample integrity. This is crucial in aerosol particulate sampling, where even small amounts of moisture can affect particle characteristics and compromise measurement accuracy.

In contrast, the Nafion dryer connected to the SMPS and CPC cannot operate in reflux mode but operates in counter-

Table 1. Technical details of the common inlets and isokinetic splitters.

Common inlet					Isokinetic splitter				
Inlet	Flow rate ($L\,min^{-1}$)	Int. (mm)	Speed diameter	Reynolds ($m\,s^{-1}$)	Instrument number	Int. diameter (mm)	Flow rate ($L\,min^{-1}$)	Reynolds number	Speed ($m\,s^{-1}$)
PM_{10}	16.7	21.2	0.8	1135	Aethalometer	8	5	885	1.6
					Nephelometer	8	5	885	1.6
					APS	4.4	1	320	1.09
$PM_{2.5}$	16.7	21.2	0.8	1135	SMPS CPC	4.4	2	655	2.2
					ToF-ACSM	8	3	530	1

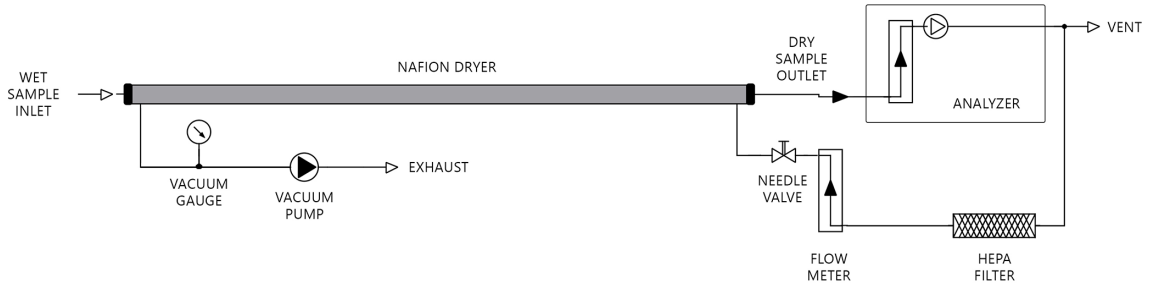

Figure 6. Schematic diagram – Nafion reflux mode (Perma Pure, 2023).

flows using dry air coming from a compressor (Acoem 8301 LC-H Zero Air Generator) since the instruments need n-butanol as a working liquid for the growth of aerosol particles (Fig. 7).

Moreover, at the inflow of each instrument, there is a high-resolution sensor connected to software for continuous monitoring (every minute) of relative humidity and temperature. The accuracy of the sensors is 2.5 % for the RH and 0.5 °C for the temperature.

Lastly, in order to limit the temperature variation around the instruments, a continuously operating air-conditioning system set at 23 °C has been installed in the laboratory.

As previously mentioned, the in situ facility is complemented by the chemical laboratory, which enables complementary measurements on the particulate-matter-loaded filters coming from the PM_x samplers, which is not possible with the continuous instrumentation. The chemical laboratory includes an inductively coupled plasma optical emission spectrophotometer (ICP-OES, series 5800, Agilent) used to perform the analysis of trace metals and a multi-wavelength OC/EC (organic carbon and elemental carbon) analyser (DRI model 2015, Magee Scientific) used to analyse the carbonaceous fraction of the collected particulate. The implementation of such a wide aerosol in situ measurement facility from scratch has required a total initial investment of about EUR 1 million and about 2 years, and about EUR 100 000 and two researchers with the support of technicians are estimated to be needed to operate the laboratory.

4.2 Instrumentation under the common PM_{10} inlet

As reported above, a PM_{10} common inlet is used to feed the aethalometer, the nephelometer, and the APS. The aethalometer is a key instrument for wildfire and pollution characterization, being capable of detecting the fraction of particulate matter which absorbs light, known as black carbon (BC), formed during the incomplete combustion of carbonaceous matter from biomass burning and fossil fuel (Petzold et al., 2013). According to the ACTRIS guidelines, the AE33 aethalometer, operating at seven different wavelengths in the range of 370–950 nm, is used for the real-time monitoring of the concentration of BC. Briefly, the principle of the aethalometer is to measure, at given time intervals, the attenuation of a light beam (at 880 nm) transmitted through a filter where the particulate matter is continuously collected; the rate of change of the optical transmission combined with the air flow rate monitored through a mass flowmeter permits one to determine the absorption coefficient, which is then converted into BC concentration by means of the mass absorption cross-section. The dual-spot technology refers to the contextual measurement of transmitted light intensities through two separate spots of the filter at different loading levels, thus allowing one to compensate for the so-called loading effect largely described by Drinovec et al. (2015). The aethalometer is equipped with a sample stream dryer (Magee Scientific) exploiting a semi-permeable Nafion membrane which keeps the RH well below 40 %.

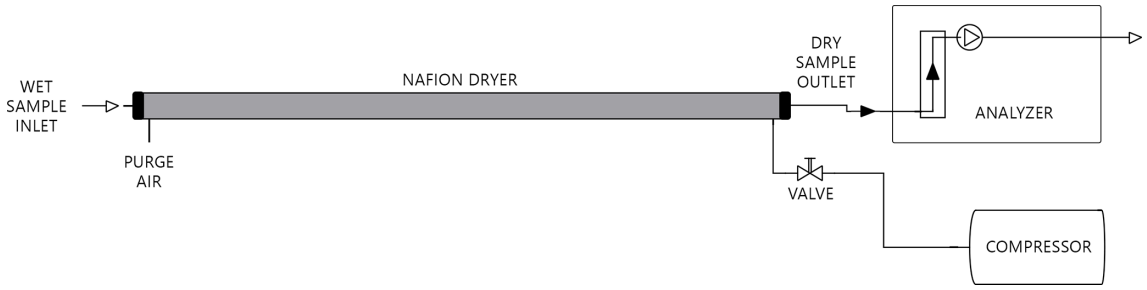

Figure 7. Schematic diagram – Nafion counter-flow mode (Perma Pure, 2023).

Among the other in situ instruments placed under the PM_{10} inlet, the nephelometer can be considered to be, in a certain way, complementary to a ground-based lidar; thus, it is expected to provide optical parameters consistent with those obtained from the lidar within the atmospheric planetary boundary layer (PBL). However, when the PBL is particularly shallow (e.g. during wintertime), the nephelometer becomes the only tool that can be used to obtain the optical parameters of the aerosol particles residing within the first hundreds of metres from the ground. The ACTRIS-compliant integrating nephelometer AURORA 3000 is used to measure the total scattering (σ_{sp}) and the backscattering (σ_{bsp}) coefficients (integrating within the angular ranges of 9–170 and 90–170°, respectively), both correlated to the particle concentration (i.e. extensive properties). The peculiarity of the instrument is the utilization of a light source being emitted at three distinct wavelengths: the light at 635 nm (red) interacts strongly with large particulate matter, such as desert dust and sea salt; the light at 525 nm (green) interacts strongly with particulate matter throughout the visible part of the electromagnetic spectrum (smog, fog, haze); and the light at 450 nm (blue) interacts strongly with fine and ultrafine particulates, such as wood fires and automobile combustion particulate. The nephelometer is equipped with a 36 in. long Perma Pure Nafion MD-700 in order to prevent condensation of water droplets over the particles, which would increase their size and significantly change their scattering characteristics.

Lastly, the APS spectrometer provides high-resolution real-time aerodynamic measurements for the coarse fraction of the particulate (Peters and Leith, 2003). The optical size range of the APS is from 0.37 to 20 µm, but since the spectrometer is connected to a PM_{10} inlet and because the counting efficiency of the APS below 0.8 µm aerodynamic diameter rapidly decreases and is unstable, the realistic size range is from 0.8 to 10 µm. The APS is based on the time-of-flight particle sizing, in which the aerodynamic size of a particle determines its rate of acceleration, with larger particles accelerating more slowly due to increased inertia; the time of flight between two laser beams is recorded and converted into aerodynamic diameter using a calibration curve. The instrument measures in parallel the light-scattering intensity of the sized particles in the equivalent optical size range from 0.8 to 10 µm, thus providing further insights into the aerosol particle nature and composition.

The APS is connected to the sampling line with only the inner nozzle (sampling 1 L min^{-1}) from the common sampling line, and the flow is dried by a 12 in. Perma Pure Nafion while taking the additional sheath flow (4 L min^{-1}) from the air compressor.

4.3 Instrumentation under the common $PM_{2.5}$ inlet

Even though the general ACTRIS recommendations for the in situ measurements involve the analysis of the PM_{10} fraction, the CPC, the SMPS, and the ACSM represent an exception and are more conveniently placed under the cut-off size of a $PM_{2.5}$ inlet. The ACTRIS-compliant CPC is used to measure the number concentration of aerosol particles with a diameter of > 10 nm. In the CPC, an aerosol sample is continuously drawn through a heated saturator where the butanol is vaporized and diffused into the sample stream. Together, the aerosol sample and *n*-butanol vapour pass into a cooled condenser, where the *n*-butanol vapour becomes supersaturated and condenses on the particle surface, causing them to grow. The particles are then counted individually as they pass through a laser-based optical detector.

Regarding the SMPS, it is an instrument of interest for CIAO, being able to provide the size distribution and concentration of the fine fraction of the particulate matter in the size range of 10–800 nm. It consists of four components in sequence: (1) a pre-impactor, which removes particles larger than the fixed upper limit in terms of size; (2) a bipolar diffusion charger (model 3082, TSI), which confers a characteristic stationary charge distribution to the polydisperse particles by using a radioactive source (Kr-85); (3) a differential mobility analyser column (DMA, model 3083, TSI), which separates the particles according to their electrical mobility by varying continuously the applied voltage within the column (Schmid et al., 2007); and (4) a condensation particle counter (CPC, model 3750, TSI) where the classified monodisperse particles are counted after the condensation of *n*-butanol on their surface.

The CPC and the SMPS are connected to the same 24 in. Perma Pure Nafion via a T-flow splitter in order to keep the

RH below 40 %. Moreover, dry sheath air is needed for the SMPS to ensure particle sizing inside the DMA with a minimum fluctuation in RH, and, for this purpose, a Silica Dryer Tube (model 3082, TSI) is incorporated into the DMA sheath flow system, which is a closed loop.

With regard to the aerosol particles mass spectrometry techniques, the ToF-ACSM has been shown to be perfectly suited for the ACTRIS observatory platforms. It is specifically designed to provide continuous aerosol particle monitoring over long time periods, spanning years, with the requirement of regular checks and calibrations to maintain the accuracy and reliability of its long-term measurements. The chemical speciation with a high temporal resolution is a unique feature of the ACSM technology, unobtainable with conventional filter sampling and subsequent post-processing chemical methods; moreover, the ACSM is not subjected to sampling artefacts that affect the collection of semi-volatile PM components by means of filters (Viana et al., 2006; Kim et al., 2015). The ToF-ACSM chosen for CIAO was introduced in 2013 (Fröhlich et al., 2013), providing a higher mass resolution (i.e. $m/\Delta m = 600$) and superior detection limits (i.e. less than nanograms per cubic metre) with respect to the previously developed quadrupole-ACSM (Ng et al., 2011) for a time resolution of 30 min. The instrument measures the mass and chemical composition of non-refractory submicron aerosol particles – i.e. organic substances, nitrates, sulfates, ammonium, and chloride – thus generating an invaluable database for the research community to characterize the particulate sources and evolution. The operational principle of the instrument is briefly described in the following: the aerosol enters the inlet where the aerodynamic lens efficiently samples and focuses submicron particles to the subsequent vacuum chamber; here, the particles impact the resistively heated porous tungsten surface at approximately 600 °C, which vaporizes the non-refractory particulate; the vaporized matter is subsequently ionized by electronic impact and is detected through the ToF analyser. In this case, the 24 in. Nafion dryer installed upstream of the instrument eliminates the complicating inlet effects due to particle-composition-dependent water uptake (Middlebrook et al., 2012).

The ACSM was installed in February 2023 and worked for some months in an almost continuous way. Then some interventions were requested to accomplish the optimization requests from the ACTRIS aerosol in situ central facility, and the ACSM restarted operations just recently in April 2024. Anyhow, the 3 months of almost continuous measurements performed in 2023 already provides some insights about aerosol particles present at the surface in Potenza. Figure 8 shows the daily concentrations of five components: chloride (Chl), ammonium (NH_4), sulfate (SO_4), nitrate (NO_3), and organic aerosol, as measured by the ACSM during the February, March, and April 2023 period (Laurita et al., 2025). Median values are preferred over mean values to avoid the strong influence of outliers and spikes in the reported values. Monthly pie charts show the relevance of the difference components for each one of the 3 months. As a general comment, we could say that the Potenza site exhibits low PM concentrations and a very high contribution of organic substances, as observed in rural areas (see, for comparison, Atabakhsh et al., 2023, and Zhao et al., 2020). The observed peaks in the total concentration, which are more pronounced in the organic component, could be related to tree pollen events typically occurring in such a period.

4.4 PM_x samplers and PM_x monitor

In addition to the online instruments report above, the field laboratory is equipped with two PM_x samplers for the continuous sampling and concentration measurement of PM_{10}, $PM_{2.5}$, and PM_1 (aerosol particles with an aerodynamic diameter of less than 1 µm) mass fractions collected over both Teflon and quartz filters; the determination of the mass of collected samples is based on the β-ray attenuation equivalent method, which strongly reduces the workload and the operator-associated variability if compared to the standard gravimetric method (Baltensperger et al., 2001). In particular, the device measures the attenuation of β rays across the filter medium which collects particulate matter, and the attenuation of the intensity in β rays is proportional to the amount of material present. Each PM_x sampler is equipped with two independent sampling lines (i.e. PM_{10} / $PM_{2.5}$ and $PM_{2.5}$ / PM_1), thus enabling the simultaneous collection of different PM fractions on independent filters. According to the workflow reported in Fig. 4, the particulate matter collected over the filters is subjected to further analysis within the chemical laboratory: the PM_{10}, $PM_{2.5}$, and PM_1 collected over 24 h on Teflon filters are analysed to determine the concentration of metals by means of the ICP-OES. On the other hand, the $PM_{2.5}$ collected over 24 h on quartz fibre filters is analysed to quantify the organic carbon (OC) and elemental carbon (EC) fractions using the thermal optical method of the OC/EC analyser; the utilization of quartz fibre filters for the OC/EC analysis is strictly recommended by the WMO/GAW 2016 guidelines, and it constitutes the only exception to the Teflon filters commonly used for other analyses. In fact, the particulate matter collected on Teflon filters is not limited to the ICP-OES analysis but can also be analysed through alternative techniques such as X-ray fluorescence (XRF) and particle-induced X-ray emission (PIXE) in order to find complementarities between the three techniques for the determination of a range of metals.

Furthermore, even if not included in the mandatory ACTRIS variables to be measured, the mass concentration for the cut-off diameters of PM_{10}, $PM_{2.5}$, and PM_1 belongs to the set of standard measurements to monitor the particulate matter, providing insight into the separation of fine and coarse particles within the aerosol.

The PM_x monitor operating at CIAO currently represents one of the main automated measurement systems for study-

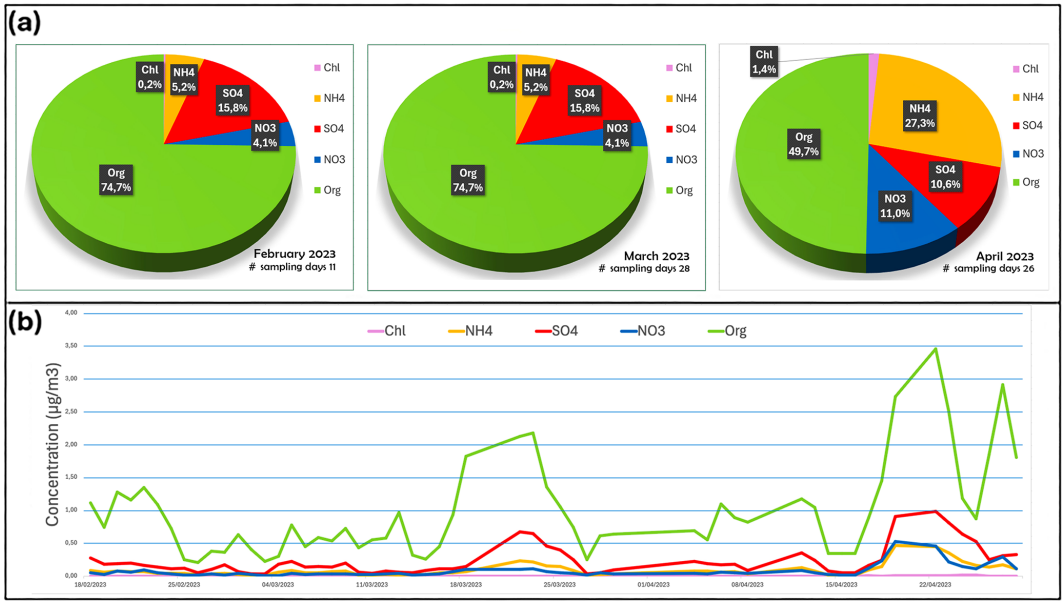

Figure 8. Daily medians of the mass fraction **(a)** and mass concentration **(b)** of each of the five chemical components of non-refractory submicron aerosol particles observed at CIAO in February–March–April 2023.

ing the concentration levels of particulate matter in ambient air. Based on the detection principle of the light scattering at the level of single particles, the system offers simultaneous real-time measurements of PM_{10}, $PM_{2.5}$, and PM_1 and particle number distributions, with a resolution of 0.1 µg m^{-3}.

4.5 Chemical laboratory

CIAO chemical laboratory is equipped with an ICP-OES and an OC/EC analyser. The ICP-OES is used to determine the qualitative and quantitative elemental composition of the metals present in the atmospheric particulate matter with high sensitivity at values below the 1 µg L^{-1} limit for certain elements. The metals are introduced into the atmosphere from various anthropogenic and natural sources. Anthropogenic metals are released into the atmosphere during combustion of fossil fuels and wood, as well as during high-temperature industrial processes and waste incineration; natural emissions result from a variety of processes acting on crustal minerals, including volcanism, erosion, surface winds, forest fires, and ocean evaporation (Allen et al., 2001; Pakkanen et al., 2001; Rajšić et al., 2008). Various metals are used as markers for the identification of emission sources: to name a few, aluminium and silicon are primarily derived from soil and rocks (crustal elements); sodium and chlorine are typically associated with marine aerosol particles; and arsenic, cadmium, manganese, and lead are mostly derived from the combustion of fossil fuels occurring at high temperatures. The ICP-OES analysis of particulate matter requires a preliminary microwave digestion of the filter in acidic conditions to extract the metals, carried out by means of a microwave digester (ETHOS UP, FKV). The obtained liquid sample is then nebulized and introduced into the plasma as an aerosol suspended in the argon gas: due to the high temperatures within the plasma (7000–10 000 K), a significant fraction of most elements exists as atoms or ions in the excited state, causing an intense polychromatic emission which continuously brings the elements back to their ground state. The polychromatic emitted light is dispersed into individual wavelengths by a polychromator and is detected by a photosensitive charge-coupled device (CCD). The concentration of each metal in the sample is obtained by using a calibration curve referenced to a solution containing the analysed elements of known concentration.

The multi-wavelength OC/EC analyser compliant with ACTRIS is used to quantify the total carbonaceous content of the particulate matter (total carbon, TC) and the OC and EC subfractions. EC is essentially a primary pollutant, emitted directly from the incomplete combustion of fossil fuels and the pyrolysis of biological material during combustion, whereas OC can be directly emitted from the incomplete combustion of organic materials and the degradation of carbon-containing products such as vegetation – primary OC – or can be produced from atmospheric reactions, involving gaseous organic precursors, i.e. secondary OC (Zhou et al., 2006). The operational principle of the thermal and/or optical analysis is based on the preferential desorption of OC and EC materials under different temperatures and atmospheres programmed within specific thermal protocols, such as the EUSAAR_2 (Cavalli et al., 2010), which is currently used within the ACTRIS community. OC usually desorbs under a non-oxidizing helium atmosphere at temperatures of up to

570 °C, while the EC is combusted in an oxidizing atmosphere with 2 % O_2 at temperatures of up to 850 °C. However, since part of the OC turns into the light-absorbing pyrolytic carbon which desorbs during the oxidizing mode, the correct discrimination between the OC and the EC fractions is conveniently identified with the point at which the light transmission reaches the pre-pyrolysis value. The liberated carbon is then completely oxidized to carbon dioxide, passing through a heated catalyst MnO_2, and is finally quantified by an NDIR (non-dispersive infrared) detector.

5 Combined deployment of aerosol remote sensing and in situ measurements

Combined approaches using aerosol particle profiling and in situ measurements are one of the most beneficial strategies in aerosol research, allowing an accurate typing and estimation of the impacts of particulate matter (Molero et al., 2020). Remote sensing techniques provide the vertical profile of the particle size distribution of the aerosol particles, as well as further physical and optical properties that are useful for understanding complex atmospheric phenomena (Vratolis et al., 2020); however, they are not able to provide information under cloudy-sky conditions or at the ground level, where the identification of aerosol particle types is only possible using the in situ instrumentation. The in-depth typing of the aerosol particles requires the information on the chemical composition, attainable only by means of in situ measurements. The complete set of data resulting from the combined approaches is crucial for identifying the sources and the evolution of the concentration levels of particulate matter over time (Bressi et al., 2021), and it is of paramount importance for the implementation of controls or policies to reduce aerosols that negatively affect air quality and public health.

The complete the picture of the aerosol particle typing, it is also necessary to clarify further the climate effects of particulate matter. In fact, the estimation of the radiative effect of atmospheric aerosol particles requires knowledge of multiple parameters, including the aerosol concentration, the optical properties, the chemical composition, the presence of clouds, and the albedo of the underlying surface. The accurate identification of aerosol particle types is also needed to improve the understanding of atmospheric dynamics and long-range transport, to improve satellite aerosol retrieval algorithms, and to validate climate models.

The multi-wavelength polarization Raman lidar is a well-established active remote sensing technique for the detection and characterization of aerosol types (Nicolae et al., 2018; Papagiannopoulos et al., 2018). Specifically, it can provide vertically resolved information on extensive (e.g. aerosol backscatter coefficient, aerosol extinction coefficient, and volume depolarization ratio) and intensive (e.g. Ångström exponent, lidar ratio, and particle depolarization ratio) aerosol optical properties. The extensive properties depend on the aerosol particle concentration, whilst the intensive properties are type-sensitive, providing information about the particle size, shape, and indices of refraction that allow for the characterization of different aerosol types. Nevertheless, the intensive properties might not be sufficient to guarantee accurate typing as some aerosol types (e.g. volcanic and desert dust particles) have very similar intensive properties but are attributed to different sources and generating mechanisms. For this reason, the discrimination of aerosol particles that typically have the same optical characteristics calls for the combined use of lidar observations and transport model simulations. The aerosol in situ observations can help in the assessment of the uncertainty of remote-sensing-retrieved products, like mass concentration, refractive index, and fine-particle concentration, obtained through inversion algorithms (e.g. Veselovskii et al., 2012; Lopatin et al., 2013).

Furthermore, the availability of collocated in situ and remote sensing measurements of aerosols also represents an added value for modelling. Indeed, it can contribute to the increase in the accuracy of model predictions, allowing for a reduction in the uncertainty of aerosol measurements in the atmosphere (e.g. Vratolis et al., 2020), as well as to a better evaluation of aerosol models. In recent years, collocated datasets have also been increasingly utilized for training machine-learning-based models, as demonstrated by Redemann and Gao (2024). To emphasize the potential synergy and added value of combining in situ and remote sensing techniques, Table 2 presents a comprehensive list of instruments and the respective parameters they measure.

In the following subsections, we present three emblematic cases recurring at CIAO, where the combined deployment of the in situ and remote sensing observations is expected to be of added value: (1) wildfires are becoming more and more relevant in the Mediterranean, especially in view of the changing climate that is expected to increase temperature, which, in turn, will affect the fires' frequency, duration, and intensity in the next decades. In this context, small and local fires are widely distributed, and their characteristics and assessment could be important at the global level. De Rosa et al. (2022) showed, with the use of lidar observations, that fresh fires can be surprisingly characterized by low absorption; this would imply a different impact of local fires in the radiation budget, which requires investigation and validation by means of in situ measurements. (2) Local pollution during winter and adverse weather can be investigated in a more exhaustive manner only by in situ observations since lidar observations provide very little information due to the generally low and unresolved-by-lidars PBL height. (3) Desert dust intrusions often reach Europe – and, especially, the Mediterranean basin – affecting local air quality, health, and ecosystem and socio-economic sectors (e.g. Monteiro et al., 2022). Given all of the above, the deployment of in situ measurements at well-equipped sites like CIAO is crucial to quantify the impact at the ground level.

Table 2. List of all CIAO remote sensing and in situ instruments and respective parameters.

	Instruments	Parameters
Cloud remote sensing	Ka-band Doppler radar, METEK MIRA-35	Vertical profiles of Doppler spectrum moments (e.g. signal-to-noise ratio, Doppler velocity, spectral width, equivalent reflectivity factor) and of linear depolarization ratio of atmospheric targets (clouds, precipitation, insects, giant aerosols). Typical measurement range: 100 m–15 km.
	Compact Ka-band Doppler radar, MIRA-35C	Same as above. Typical measurement range: 100 m–12 km
	W-band Doppler radar, RPG-FMCW-94	Same as above. Typical measurement range: 50 m–12 km.
	K-band Doppler radar, METEK MRR-PRO	Vertical profiles of hydrometeors' Doppler spectrum moments, raindrop size distribution, liquid-water mass concentration, and rain rate. Typical measurement range: 15 m–6 km.
	Microwave radiometer, RPG-HATPRO-G5	Vertical profiles of temperature, humidity, and cloud liquid-water mass concentration; integrated precipitable water vapour and cloud liquid-water path. Typical measurement range: 0–10 km.
	Ceilometer, Vaisala CL51	Vertical profiles of attenuated backscatter coefficient from atmospheric particles (aerosols, clouds, and precipitation), cloud base heights, and aerosol vertical layering. Typical measurement range: from near surface (15 m) up to 12 km for clouds, depending on the aerosol load in a cloud-free atmosphere.
	Ceilometer, Vaisala CL31	Same as above. Typical measurement range: from near surface (15 m) up to 8 km for clouds, depending on the aerosol load in a cloud-free atmosphere.
	Ceilometer, Lufft CHM15k	Same as above. Typical measurement range: from near surface (15 m) up to 15 km for clouds, depending on the aerosol load in a cloud-free atmosphere.
	Two Doppler lidars, HALO Photonics StreamLineXR	Vertical profiles of attenuated backscatter coefficient from atmospheric particles (aerosols, clouds, and precipitation) and of vertical and horizontal wind components.
Trace gas remote sensing	FTIR, Bruker 125HR	Infrared spectrum containing the signatures of vibrational–rotational transitions of numerous trace gases in the terrestrial atmosphere as they absorb solar radiation (O_3, HCl, HF, $ClONO_2$, HNO_3, N_2O, CH_4, CO, C_2H_6, and HCN).
Aerosol remote sensing	Fixed multi-wavelength Raman lidar	Aerosol extinction coefficients at 355 and 532 nm; aerosol backscatter, volume, and particle depolarization ratio at 355, 532, and 1064 nm and water vapour mixing ratio.
	Mobile multi-wavelength Raman lidar	Aerosol extinction coefficients at 355 and 532 nm; aerosol backscatter, volume, and particle depolarization ratio at 355, 532, and 1064 nm.
	MUSA Transportable Fixed multi-wavelength Raman lidar	Aerosol backscatter at 355, 532, and 1064; aerosol extinction coefficients at 355 and 532 nm; volume and particle depolarization ratio at 532.
	Scanning UV Raman lidar	Aerosol backscatter, aerosol extinction coefficients, volume and particle depolarization ratio at 355.
	Automatic sun, sky, and lunar photometer, Cimel 318T	Aerosol optical depth (AOD), volume size distribution (VSD), complex refractive index (n), shape factor, water vapour content.

Table 2. Continued.

	Instruments	Parameters
Aerosol in situ	SMPS	Size distribution and concentration of the particles in the size range 10–800 nm.
	APS	Size distribution and concentration of the particles in the size range 0.8–10 µm.
	CPC	Concentration of the number of particles with dimensions of > 10 nm.
	Nephelometer	Aerosol scattering and backscattering coefficients at 450, 525, and 635 nm.
	Aethalometer	Aerosol absorption coefficients and BC concentration at seven wavelengths in the range of 370–950 nm.
	PM_x monitor	Mass concentration for the cut-off diameters of PM_{10}, $PM_{2.5}$, and PM_1.
	ACSM	Real-time chemical characterization of the main organic and inorganic components of the non-refractory sub-micrometric aerosol particles.
	ICP-OES	Qualitative and quantitative elemental composition of the metals on collected filters of aerosol particles.
	OC/EC analyser	TC and subfraction OC/EC concentrations on collected filters of aerosol particles.

5.1 Local wildfires

The study of smoke from wildfires spreading over short distances represents a great example for a synergistic approach based on remote sensing and in situ techniques. In such a case, the smoke particles spread mainly at low levels and deposit quickly on the ground, where in situ measurements are the only tool able to provide reliable information to support and integrate what is observed above medium-overlap regions, a prerogative of remote sensing techniques.

The multi-wavelength polarization Raman lidar is a well-known tool to study smoke layers in the atmosphere, being able to separate aerosols according to their specific optical signature (Ohneiser et al., 2021). Specifically, a sign of the dominance of smoke in the aerosol layer is the aerosol extinction-to-backscatter ratio (the so-called lidar ratio, S) at 532 and 355 nm, which is typically high (i.e. > 50 sr) as a consequence of the presence of absorbing BC produced during biomass burning; moreover, the ratio of S measured at the different wavelengths may be used as an indicator of the phase of the ongoing wildfire (e.g. Nicolae et al., 2013). Other lidar parameters largely used to investigate the smoke are the particle linear depolarization ratio (PLDR) and the Ångström exponent (AE), which provide information about the shape and the size of the particles, respectively. In the case of a local wildfire, the observation of quasi-spherical and relatively small particles is expected since the newly produced smoke particles do not have the time to undergo modifications during transport.

The Ångström absorption and scattering exponents (AAE and SAE) – derived from the aethalometer and nephelometer measurements, respectively – provide the optical typing of the smoke, with the value of the AAE being expected to correlate with the lidar observations (Cazorla et al., 2013) and, therefore, with the nature of spreading fire.

Among the aerosol in situ instruments, the aethalometer is crucial to study smoke produced during wildfires, being able to quantify the BC that originated from the incomplete combustion of carbonaceous matter and providing an estimate of the biomass burning (BB) apportionment to the overall BC (Sandradewi et al., 2008). Additionally, the OC/EC thermal and/or optical analysis of the $PM_{2.5}$ fraction is very important because the increase in organic carbon and elemental carbon concentrations has been the most indicated element reflecting wildfire emissions. Fine particles (≤ 2.5 µm) are a major pollutant from wildfire smoke. Key in situ analyses include size distribution and concentration measurements using SMPS and CPC as fine particles are more abundant during fires compared to during other periods. Real-time PM_x monitoring confirms increases in $PM_{2.5}$ / PM_{10} and PM_1 / $PM_{2.5}$ ratios during fire events. Finally, the in situ investigation of wildfire smoke is completed by the chemical analysis obtained with the ToF-ACSM: in particular, key tracers of biomass burning organic aerosol particles in mass spectra are the enhanced signals at $m/z60$ and 73, at-

tributable to $C_2H_4O_2^+$ and $C_3H_5O_2^+$ ions, respectively, coming from the fragmentation of the so-called "levoglucosan-like" species originating from the pyrolysis of cellulose (Cubison et al., 2011). Finally, the chemical analysis of the filters through the ICP-OES is fundamental for tracking the levels of potentially toxic elements (PTEs) such as As, Sb, Cd, Hg, Pb, Cr, Cu, Ni, Se, Tl, Sn, V, and Zn. This monitoring is vital as these elements have the potential to be released into the environment during wildfires, posing a threat to humans and animals when their absorbed doses surpass the established reference values (Pacifico et al., 2023).

This case underlines the critical need for a combined approach, where in situ measurements bridge the gap and enhance the interpretation of remote sensing data, showcasing the strength of CIAO's integrated monitoring capabilities.

5.2 Local pollution in wintertime

Winter months commonly exhibit heightened air pollution levels, primarily attributable to temperature inversions. Inversion occurrences involve a layer of warm air confining colder air and pollutants close to the ground, impeding their dispersion into the atmosphere. Unlike summer air pollution, winter conditions result in the prolonged presence of pollutants, increasing the likelihood of higher inhalation rates. This extended exposure raises health concerns for individuals as reduced ventilation and dispersion contribute to potential health effects.

Air quality near the ground during winter is expected to be dominated by local residential heating emissions with the contribution of vehicle engine exhausts. For this season, the in situ measurements represent the most viable way to investigate the aerosol particle distribution and composition, while the deployment of remote sensing instruments (e.g. lidar) is limited by instrumental and environmental factors. During wintertime, the condensation of water droplets (especially during nighttime), along with the recurrent formation of cloud layers, attenuates the laser beam, thus impeding the lidar retrievals; moreover, even under clear-sky conditions, the particulate is usually confined within the first 300 m from the ground (i.e. the typical PBL layer thickness in wintertime), where the active remote sensing techniques are not able to provide reliable results because of the typical overlap between laser beam and receiving systems in lidar at this vertical range .

The climatological profile of aerosol backscatter at 532 nm for the winter seasons of 2000–2019 at CIAO (blue line in Fig. 9) shows very clean air with respect to other seasons in the whole investigated atmospheric column (https://doi.org/10.57837/cnr-imaa/ares/actris-earlinet/level3/climatological/2000_2019/pot, Mona et al., 2024).

Only the last point close to the surface is slightly higher with respect to the other seasons, but the information content is too low for further investigation. These cases are typically

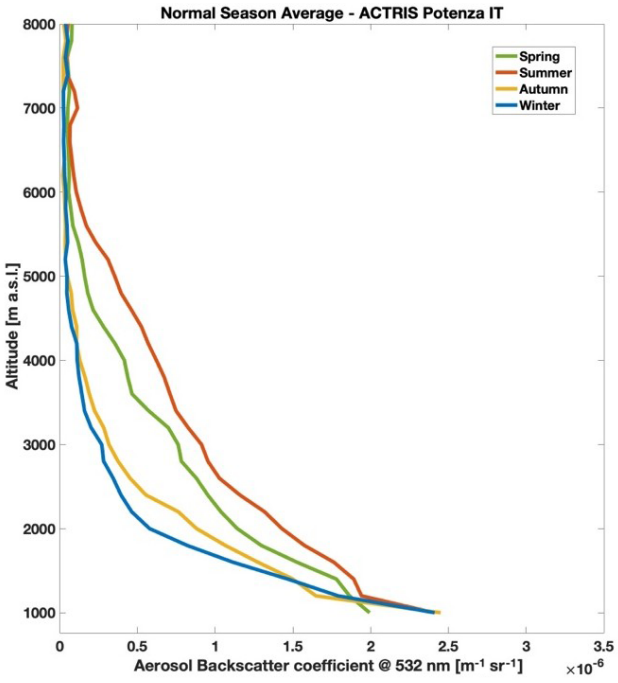

Figure 9. Climatological profiles of the aerosol backscatter at 532 nm observed at CIAO from 2000 to 2019. Normal season average is reported: each profile is the average of all aerosol backscatter profiles observed at CIAO for each season in routine measurements collected from 2000 to 2019.

considered to be clean days from the aerosol remote sensing perspective. However, it must be noted that the lidar is blind to the lowest portion of the atmosphere, where pollutants are concentrated due to the low boundary layer height (PBL).

On the other hand, only the in situ measurements, which do not see above the boundary layer height, can capture well what is happening close the surface.

In this context, we investigate the average daily concentration of elemental carbon (eBC) obtained by the aethalometer (Fig. 10a), covering the period from June 2023 to April 2024 (Laurita et al., 2025), to gain first insights into air quality near the ground during winter. Our analysis reveals no significant increase in eBC concentration during the winter months compared to the background levels observed in summer. However, when examining the daily average percentage of black carbon (BC) originating from biomass burning (BB%) (Laurita et al., 2025), as determined by the Sandradewi model (Sandradewi et al., 2008), in conjunction with the daily average temperature data obtained from the Vaisala AWS310 weather station situated at the site (Fig. 10b), an intriguing trend emerges. It becomes evident that BB% is substantially higher during winter months than during summer months. Given the minimal occurrence of wildfires and prescribed burns at the site during winter, the primary source of biomass burning influence can be attributed to residential burning, a

consequence of the notably low temperatures experienced during that period.

These initial data indicate that the main source of BC during winter at our site is predominantly from local residential heating emissions. Unlike remote sensing, which may suggest clean air conditions, in situ measurements reveal significant pollution at the ground level, underscoring that winter cases should not be considered to be background conditions in the boundary layer region. Therefore, this preliminary study demonstrates that combining remote sensing and in situ measurements provides critical insights that neither method can achieve independently.

Future studies could expand on this by incorporating additional in situ instruments alongside the aethalometer.

For example, OC/EC analysis on the $PM_{2.5}$ fraction could support and complement aethalometer results (Schmidl et al., 2008; Gonçalves et al., 2010; Pio et al., 2011; Sirignano et al., 2019), while a nephelometer could provide ground-level optical parameters, such as the scattering coefficient (σ_{sp}) and backscattering coefficient (σ_{bsp}), which are linked to particle concentrations, particularly fine and ultrafine particles typical of heating emissions (Esteve et al., 2012).

The ToF-ACSM could offer a detailed chemical composition of PM_1, expected to reveal a dominance of organic matter from combustion processes. Secondary ammonium nitrate (NH_4NO_3), associated with residential wood burning and diesel emissions (via NO_x), could also explain exceedances in fine-particle fractions during winter (Chen et al., 2012).

Finally, filter analysis with the ICP-OES could identify metals in the particulate matter (e.g. Na, Mg, Zn, Pb) originating from specific sources such as fossil fuel and biomass combustion, vehicular traffic, and dust resuspension (Dušan et al., 2017; Zhi et al., 2021). This in situ multi-instrument approach would provide a comprehensive view of particulate composition and sources during winter pollution episodes at the surface, enabling a deeper insight into winter aerosol conditions, addressing air quality challenges, and accurately evaluating their health impacts.

5.3 Dust intrusions

During summer and spring, the site is regularly affected by Saharan dust intrusions (Mona et al., 2006). Desert dust particles have many effects: they can impact climate, the precipitation cycle, and human health (Sokolik and Toon, 1996; Mona et al., 2023). Mineral dust particles can act as cloud condensation nuclei (CCN) and thereby determine the concentration of the initial droplets, albedo, precipitation formation, and lifetime of clouds (Levin et al., 1996, 2005).

The multi-wavelength polarization Raman lidar provides highly resolved spatial and temporal atmospheric profiles that allow for the separation of the different aerosol layers (Pappalardo et al., 2004b; Papagiannopoulos et al., 2018). Large and irregularly shaped Saharan desert dust particles produce medium lidar ratios and relatively high PLDR values, and they are spectrally neutral to backscatter and extinctions producing low Ångström exponents within the wavelengths 355–532 nm (Freudenthaler et al., 2009; Fernandez et al., 2019). In fact, mineral desert dust aerosol particles predominantly consist of coarse-mode particles of irregular shapes (Mahowald et al., 2014).

In situ measurements, in the case of sedimentation events, provide complementary information on the advected dust. Low values of nephelometer-derived SAE indicate coarse particles, and, conversely, high aethalometer-derived AAE values demonstrate the wavelength-dependent absorption (Cazorla et al., 2013).

During dust-dominated atmospheric conditions, sedimentation increases, returning large particles to the ground. The APS size distribution measurements of coarse particles are crucial for dust studies. A low $PM_{2.5}$ / PM_{10} ratio from real-time PM_x monitoring data confirms the dominance of the coarse fraction during desert dust events. Additionally, 24 h PM_{10} mass concentrations measured by the PM_x sampler (SWAM 5a Dual Channel Monitors, FAI Instruments) are higher during dust events, often exceeding the European daily limit (2008/50/CE European directive).

For chemical characterization, the ICP-OES detects the mineral fraction's elemental composition, particularly crustal elements like Al, Ca, Fe, K, and Na, along with rare Earth elements (REEs). These concentrations are significantly elevated during dust events compared to annual averages (Aydin et al., 2012; Rodriguez-Navarro et al., 2018; Mărmureanu et al., 2019).

In the following, we report on an example of aerosol remote sensing and in situ observation for a Saharan dust intrusion at CIAO to demonstrate the possibilities for a complementary combination of data from lidar and in situ aerosol measurements. Even if only the APS instrument was available at that time, the presence of just one in situ instrumentation already shows the importance of such a combination of techniques. The observations are related to the second half of June. Figure 11a reports on the fine-mode fraction as retrieved from CIAO photometer measurements and available at NASA Goddard Space Flight Center (2024). This parameter provides information about the fraction of fine-mode particles respect to the coarse-mode fraction as obtained from the AOD (aerosol optical depth) measurements. This parameter is retrieved from columnar measurements and therefore refers to the total atmospheric column. Figure 11a clearly shows that, in the 20–23 June period, the coarse particles are more abundant with respect to the previous and following periods. For the same period, Hybrid Single-Particle Lagrangian Integrated Trajectory (HYSPLIT) backward trajectories ending over Potenza indicate Sahara desert as a potential source of the observed particles.

Lidar observations provide better insight into the temporal and vertical distribution of the aerosol particles at CIAO on those days. Figure 11b–c report on available lidar observa-

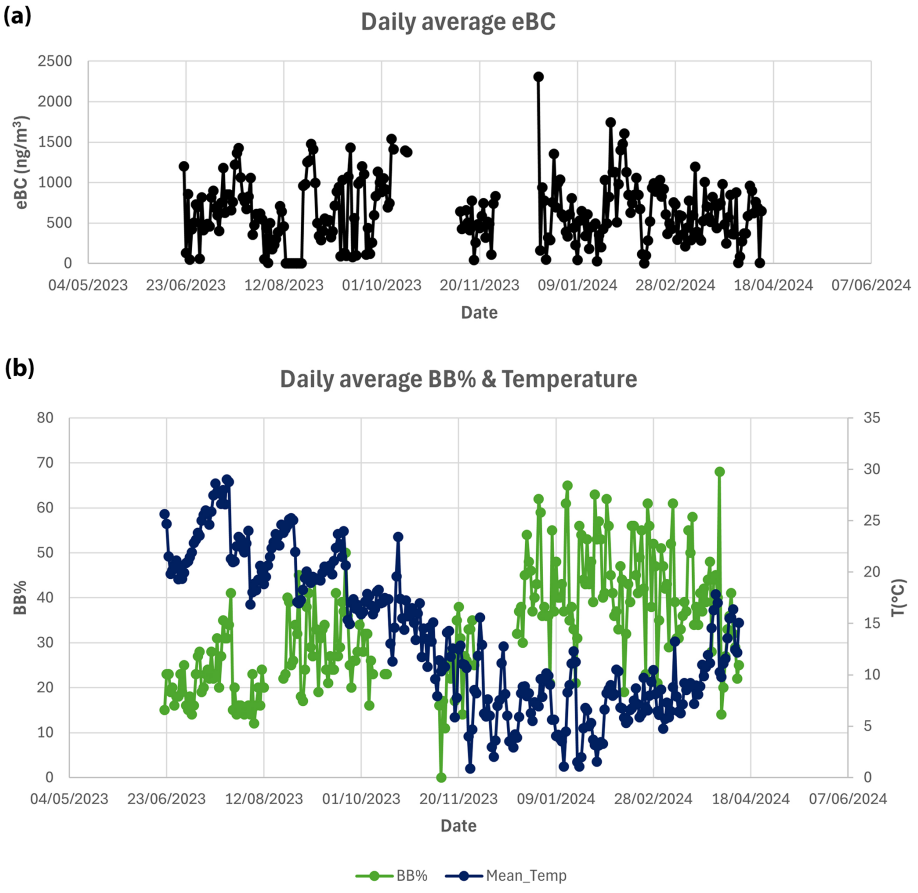

Figure 10. Daily average eBC concentration obtained by aethalometer from June 2023 to April 2024 **(a)** and daily average BB% determined by the Sandradewi model and daily average temperature data obtained from the Vaisala AWS310 weather station from June 2023 to April 2024 **(b)**.

tions for the period (ACTRIS Data Centre, 2023). It shows the colour maps of the vertical distribution and the temporal dynamics of the aerosol as time series of range-corrected lidar signals at 532 nm for the night of 22 June 2023 and during the daytime of 23 June 2023. In particular, these plots display the component of the backscattered signal at 532 nm that is cross-polarized, which is polarized perpendicular to the emitted laser light: the presence of highly cross-polarized backscatter signals is a signature of the presence of aspherical particles in that portion of the 4D atmospheric region, e.g. Saharan dust particles.

The representation of the aerosol particle distribution during the night of 22 June (Fig. 11b) shows two main layers of dust: one at an altitude close to 1 km above ground level (a.g.l.) and a second denser one above it at a height of approximately 3 km a.g.l. Particularly interesting for the potential link with in situ measurements is a branch of the lower layer around 01:30 UTC between 22 and 23 June, which seems to descend in altitude and could potentially sediment at the ground. It is worth noting that the lidar blind region for the instrument available at the time of the measurements was around 400 m, not allowing us to investigate further beyond point. Over the next day (Fig. 11c), the colour map again indicates the presence of dust from 09:00 to 12:00 UTC at similar heights compared to 22 June but with lower density until disappearing after 12:00 UTC.

Online observations on the ground allow for a better understanding of the dust presence at the surface and also for exploring the status after the 22–23 June. In that period, only the APS and aethalometer were operational at CIAO.

Figure 11d shows the aerodynamic particle size distribution daily averages obtained with the APS on 22–25 June 2023 (Laurita et al., 2025) and provides information complementary to that obtained through lidar and photometer measurements. Indeed, Fig. 11d distinctly illustrates that there is negligible variance in the concentration of ultrafine particulates between dust (22–23 June) and non-dust (24–25 June) days; instead, there is a noticeable rise in the concentration of fine and coarse particles with diameters of up to 5 µm on the dust days (22–23 June) compared to on the non-dust days (24–25 June); demonstrating how, during dust events, the atmosphere is dominated by large particles

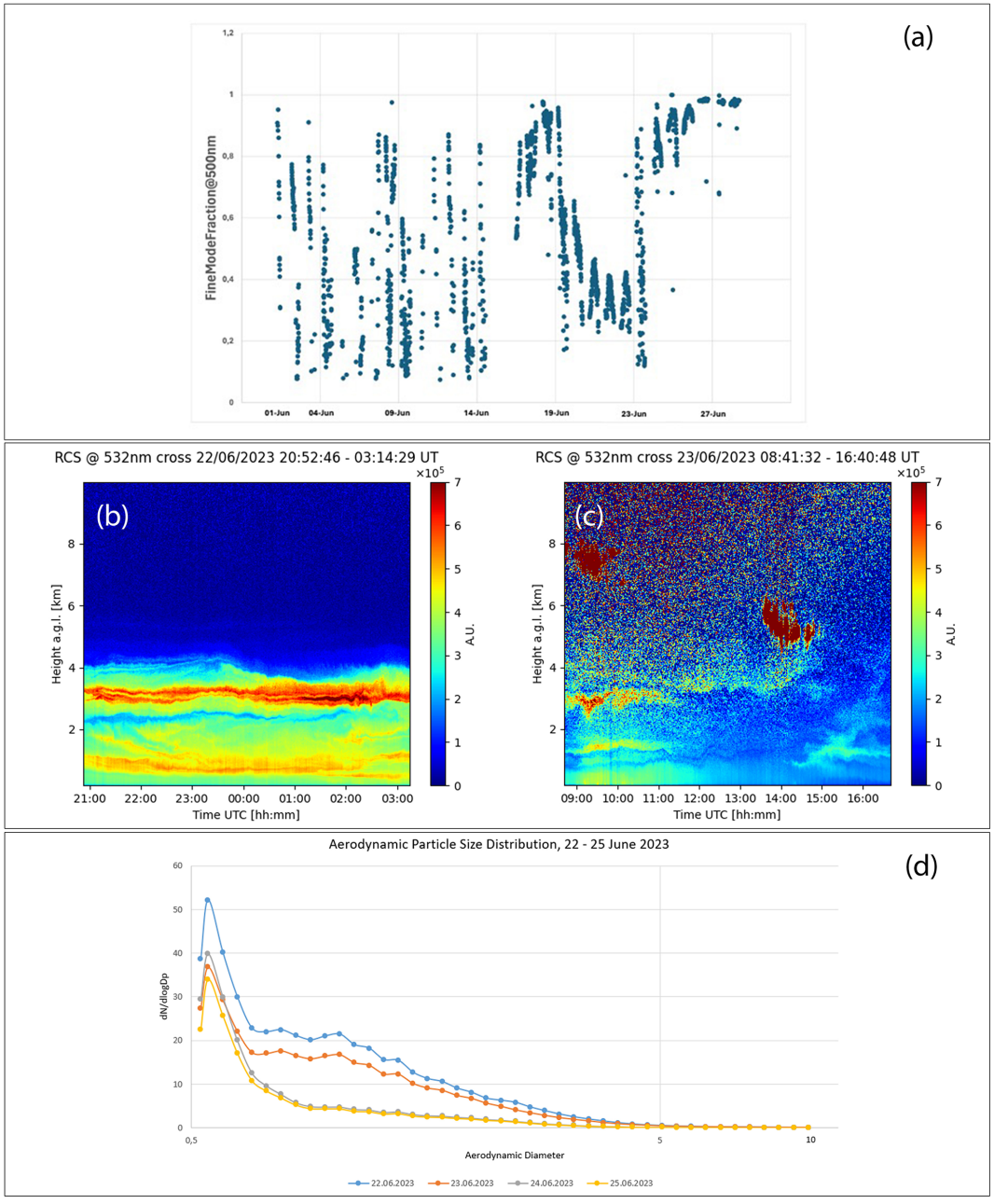

Figure 11. Fine-mode fraction as retrieved from CIAO photometer measurements related to the second half of June **(a)**, colour-coded time series of range-corrected lidar signals measured at 532 nm cross-polarized channel obtained with the MUSA lidar system on 22 June 2023 **(b)** and on 23 June 2023 **(c)**, and aerodynamic particle size distribution daily averages obtained with APS on 22–25 June 2023 **(d)**.

(Fig. 11a) distributed over different altitude ranges (Fig. 11b–c) and if sedimentation is favoured, this leads to a greater return to ground level in the coarse mode (Fig. 11d).

This case demonstrates strong agreement between remote sensing and in situ measurements in identifying and characterizing a desert dust event. The lidar provides a detailed vertical and temporal distribution of aerosols, while in situ measurements capture surface-level dynamics, overcoming the lidar's limitations in the blind region near the ground. Together, these methods reveal a more complete picture of the dust event.

Future synergistic products could involve integrating additional in situ instruments with remote sensing to provide richer data for events like this. For example, upgraded systems at CIAO, including advanced offline and online instruments, will enable deeper analyses of similar phenomena. While a detailed investigation of this event is beyond the scope of this paper, it sets the foundation for future stud-

ies exploring the full potential of these complementary approaches.

6 Conclusions

The recent upgrade of CIAO with an aerosol in situ laboratory, in addition to the well-established remote sensing instrumentation, significantly enhances its observational capacity. The integration of in situ and remote sensing measurements offers a more complete understanding of aerosol behaviour, enabling detailed studies from the ground level up to the stratosphere. This combination adds value by providing both vertical profiles by remote sensing measurements and precise ground-level chemical and physical properties through in situ measurements, which is crucial for improving climate models and understanding aerosol impacts on human health.

Establishing the aerosol in situ facility has been a complex and labour-intensive endeavour. The process, which began in 2018, required careful planning, technical expertise, and collaboration with field specialists. The setup involved designing and implementing ACTRIS-compliant inlets, sampling lines, and advanced instruments to ensure accurate and reliable measurements. This development highlights the significant effort required to meet international standards and to provide high-quality data for the scientific community.

Given CIAO's strategic location in the Mediterranean, the case studies planned for future research are especially relevant. The site is frequently affected by Saharan dust intrusions, which impact air quality and ecosystems, and the observatory is strategically positioned to study these phenomena. Moreover, the Mediterranean is also prone to wildfires, which are projected to increase in intensity and frequency due to climate change. CIAO can monitor both the short-range transport of smoke from local fires and long-range plumes from major events, providing insights into their effects on air quality and human health. Lastly, local winter pollution, which results from residential heating, can also be analysed in detail, particularly during temperature inversions that trap pollutants near the ground. The combination of in situ and remote sensing measurements will help investigate these key environmental issues.

Furthermore, the next-to-come ICOS Atmospheric Class 1 site at CIAO (first step of labelled process already passed) will offer other possibilities in terms of synergistic studies and integration among RIs in the environmental field. In this direction, CIAO is deeply involved in the development of ITINERIS (Italian Integrated Environmental Research Infrastructures System), an overarching national project for enhancing the interlinkages of all the Italian RIs in the environmental domain. The multi-platform and multi-disciplinary approach of the observatory, coupled with the open data and open-access philosophy, is key for better addressing complex atmospheric and environmental questions posed by climate change and anthropization processes.

Appendix A: List of abbreviations

AAE	Ångström absorption exponent
ACTRIS	Aerosol, Clouds and Trace gases Research Infrastructure
AE	Ångström exponent
AERONET	Aerosol Robotic Network
APS	Aerodynamic particle sizer
BB	Biomass burning
BC	Black carbon
CCD	Charge-coupled plasma
CIAO	CNR-IMAA (Consiglio Nazionale delle Ricercahe-Istituto di Metodologie per l'Analisi Ambientale) Atmospheric Observatory
CNN	Cloud condensation nuclei
CPC	Condensation particle counter
DMA	Differential mobility analyser
EARLINET	European Aerosol Research Lidar Network to Establish an Aerosol Climatology
eBC	Equivalent black carbon
EC	Elemental carbon
FTIR	Fourier-transform infrared spectroscopy
GALION	GAW Aerosol Lidar Observation Network
GAW	Global Atmosphere Watch
GCOS	Global Climate Observing System
GRUAN	GCOS Reference Upper-Air Network
HYSPLIT	Hybrid Single-Particle Lagrangian Integrated Trajectory
ICOS	Integrated Carbon Observing System
ICP-OES	Inductively coupled plasma emission spectrophotometer
NDIR	Non-dispersive infrared
OC	Organic carbon
PBL	Planetary boundary layer
PIXE	Particle-induced X-ray emission
PLDR	Particle linear depolarization ratio
PM	Particulate matter
RH	Relative humidity
RI	Research infrastructure
SAE	Ångström scattering exponent
SMEs	Small- and medium-sized enterprises
SMPS	Scanning mobility particle sizer
TC	Total carbon
ToF-ACSM	Time-of-flight aerosol chemical speciation monitor
WMO	World Meteorological Organization
XRF	X-ray fluorescence

Code availability. The code related to this article is available upon request to the corresponding author.

Data availability. The lidar data are accessible via the REST API interface provided by the ACTRIS EARLINET Data Portal at https://data.earlinet.org/api/swagger-ui/# (ACTRIS Data Centre, 2023). The specific lidar datasets used in this study, along with the corresponding query results, are available upon request from the corresponding author. The ACSM, APS, and aethalometer data used in this study are available through the ITINERIS HUB data repository (https://doi.org/10.71763/2KZ1-X145, Laurita et al., 2025). The aerosol optical data used in this study are available via the AERONET website (https://aeronet.gsfc.nasa.gov, NASA Goddard Space Flight Center, 2024). The other data related to this article are available upon request from the corresponding author.

Author contributions. TL, AM, and ST contributed to writing the paper (original draft preparation). TL, AM, ST, CCol, and MM contributed to the visualization. TL, AM, ST, FC, and DA contributed to the methodology. TL and MM contributed to the formal analysis. DA, AG, CD, ER, and CC contributed to the resources. CCor, SG, RMPA, and GP contributed to the funding acquisition. EL contributed to the software. TL, AM, ST, AA, BDR, MR, and LM contributed to the writing of the paper (review and editing). FC, EL, FM, DA, AG, CCor, BDR, CD, SG, MM, NP, GP, RMPA, ER, DS, and CCol contributed to the review and editing. GP and LM contributed to the conceptualization. LM contributed to the project administration and supervision.

Competing interests. The contact author has declared that none of the authors has any competing interests.

Disclaimer. Publisher's note: Copernicus Publications remains neutral with regard to jurisdictional claims made in the text, published maps, institutional affiliations, or any other geographical representation in this paper. While Copernicus Publications makes every effort to include appropriate place names, the final responsibility lies with the authors.

Acknowledgements. The authors acknowledge the team of the ACTRIS Topical Centre CAIS-ECAC (Centre for Aerosol In Situ Measurements–European Center for Aerosol Calibration and Characterization) for their detailed advice and individual help in setting up the aerosol in situ measurement programme according to the ACTRIS standard procedures.

Financial support. This research has been supported by ITINERIS, the Italian Integrated Environmental Research Infrastructure System (grant no. IR0000032, D.D. no. 130/2022 – CUP B53C22002150006), which is funded by the European Union under Next Generation EU – PNRR Mission 4, Component 2, Investment 3.1: Fund for the realization of an integrated system of research and innovation infrastructures; ATMO-ACCESS (Access to Atmospheric Research Facilities), which is funded as part of the Horizon 2020 programme (H2020-EU.1.4.1.2) by the European Union (grant no. 101008004, 1 April 2021–31 March 2025); PER-ACTRIS-IT (Potenziamento della componente italiana della Infrastruttura di Ricerca Aerosol, Clouds, and Trace Gases Research Infrastructure), – Avviso MUR D.D. no. 2595 del 24.12.2019 Piano Stralcio "Ricerca e Innovazione 2015–2017", PIR01_00015, CUP B17E19000000007, and CIR01_00015, CUP F88I2000019000, which is funded by the European Regional Development Fund – MIUR (Italian Ministry of University and Research); and the Joint Research Unit ACTRIS Italy, D. M. no. 571 del 21-6-2022, Fondo ordinario per gli enti e le istituzioni di ricerca (FOE) 2022 and D. M. no. 789 del 21-06-2023 Fondo ordinario per gli enti e le istituzioni di ricerca (FOE) 2023, which is funded by MIUR (Italian Ministry of University and Research).

Review statement. This paper was edited by Hartmut Herrmann and reviewed by two anonymous referees.

References

ACTRIS: Aerosol, Clouds and Trace Gases Research Infrastructure, https://www.actris.eu, last access: 13 December 2023.

ACTRIS Data Centre: EARLINET Lidar Data Access via REST API, https://data.earlinet.org/api/swagger-ui/#, last access: 20 December 2023.

ATMO-ACCESS: Second Call for Access, https://www.atmo-access.eu/second-call-for-access/, last access: 2 December 2023.

Allen, A. G., Nemitz, E., Shi J. P., Harrison R. M., and Greenwood, J. C.: Size distribution of trace metals in atmospheric aerosols in the United Kingdom, Atmos. Environ., 35, 4581–4591, https://doi.org/10.1016/S1352-2310(01)00190-X, 2001.

Aydin, F., Aydin, I., Erdoğan, S., Akba, O., Isik, B., and Hamamci, C.: Chemical Characteristics of Settled Particles during a Dust-Storm, Pol. J. Environ. Stud., 21, 533–537, 2012.

Atabakhsh, S., Poulain, L., Chen, G., Canonaco, F., Prévôt, A. S. H., Pöhlker, M., Wiedensohler, A., and Herrmann, H.: A 1-year aerosol chemical speciation monitor (ACSM) source analysis of organic aerosol particle contributions from anthropogenic sources after long-range transport at the TROPOS research station Melpitz, Atmos. Chem. Phys., 23, 6963–6988, https://doi.org/10.5194/acp-23-6963-2023, 2023.

Baars, H., Ansmann, A., Ohneiser, K., Haarig, M., Engelmann, R., Althausen, D., Hanssen, I., Gausa, M., Pietruczuk, A., Szkop, A., Stachlewska, I. S., Wang, D., Reichardt, J., Skupin, A., Mattis, I., Trickl, T., Vogelmann, H., Navas-Guzmán, F., Haefele, A., Acheson, K., Ruth, A. A., Tatarov, B., Müller, D., Hu, Q., Podvin, T., Goloub, P., Veselovskii, I., Pietras, C., Haeffelin, M., Fréville, P., Sicard, M., Comerón, A., Fernández García, A. J., Molero Menéndez, F., Córdoba-Jabonero, C., Guerrero-Rascado, J. L., Alados-Arboledas, L., Bortoli, D., Costa, M. J., Dionisi, D., Liberti, G. L., Wang, X., Sannino, A., Papagiannopoulos, N., Boselli, A., Mona, L., D'Amico, G., Romano, S., Perrone, M. R., Belegante, L., Nicolae, D., Grigorov, I., Gialitaki, A., Amiridis, V., Soupiona, O., Papayannis, A., Mamouri, R.-E.,

Nisantzi, A., Heese, B., Hofer, J., Schechner, Y. Y., Wandinger, U., and Pappalardo, G.: The unprecedented 2017–2018 stratospheric smoke event: decay phase and aerosol properties observed with the EARLINET, Atmos. Chem. Phys., 19, 15183–15198, https://doi.org/10.5194/acp-19-15183-2019, 2019.

Baltensperger, U., Weingarter, E., Burtscher, H., and Keskinen, J.: Dynamic mass and surface area measurements, in: Aerosol Measurement, edited by: Baron, P.-A., and Willeke, K., Jon Wiley and Sons, New York, 387–418, ISBN 978-0-471-35636-3, 2001.

Binietoglou, I., Basart, S., Alados-Arboledas, L., Amiridis, V., Argyrouli, A., Baars, H., Baldasano, J. M., Balis, D., Belegante, L., Bravo-Aranda, J. A., Burlizzi, P., Carrasco, V., Chaikovsky, A., Comerón, A., D'Amico, G., Filioglou, M., Granados-Muñoz, M. J., Guerrero-Rascado, J. L., Ilic, L., Kokkalis, P., Maurizi, A., Mona, L., Monti, F., Muñoz-Porcar, C., Nicolae, D., Papayannis, A., Pappalardo, G., Pejanovic, G., Pereira, S. N., Perrone, M. R., Pietruczuk, A., Posyniak, M., Rocadenbosch, F., Rodríguez-Gómez, A., Sicard, M., Siomos, N., Szkop, A., Terradellas, E., Tsekeri, A., Vukovic, A., Wandinger, U., and Wagner, J.: A methodology for investigating dust model performance using synergistic EARLINET/AERONET dust concentration retrievals, Atmos. Meas. Tech., 8, 3577–3600, https://doi.org/10.5194/amt-8-3577-2015, 2015.

Boselli, A., Caggiano, R., Cornacchia, C., Madonna, F., Macchiato, M., Mona, L., Pappalardo, G., and Trippetta, S.: Multi year sun-photometer measurements for aerosol characterization in a Central Mediterranean site, Atmos. Res., 104, 98–110, https://https://doi.org/10.1016/j.atmosres.2011.08.002, 2012.

Bressi, M., Cavalli, F., Putaud, J. P., Fröhlich, R., Petit, J. E., Aas, W., Äijälä, M., Alastuey, A., Allan, J. D., Aurela, M., Beric, M., Bougiatioti, A., Bukowiecki, N., Canonaco, F., Crenn, V., Dusanter, S., Ehn, M., Elsasser, M. and Prevot, A. S. H.: A European aerosol phenomenology – 7: High-time resolution chemical characteristics of submicron particulate matter across Europe, Atmos. Environ., 10, 100108 https://doi.org/10.1016/j.aeaoa.2021.100108, 2021.

Cavalli, F., Viana, M., Yttri, K. E., Genberg, J., and Putaud, J.-P.: Toward a standardised thermal-optical protocol for measuring atmospheric organic and elemental carbon: the EUSAAR protocol, Atmos. Meas. Tech., 3, 79–89, https://doi.org/10.5194/amt-3-79-2010, 2010.

Cazorla, A., Bahadur, R., Suski, K. J., Cahill, J. F., Chand, D., Schmid, B., Ramanathan, V., and Prather, K. A.: Relating aerosol absorption due to soot, organic carbon, and dust to emission sources determined from in-situ chemical measurements, Atmos. Chem. Phys., 13, 9337–9350, https://doi.org/10.5194/acp-13-9337-2013, 2013.

Chen, L.-W. A., Watson, J. G., Chow, J. C., Green, M. C., Inouye, D., and Dick, K.: Wintertime particulate pollution episodes in an urban valley of the Western US: a case study, Atmos. Chem. Phys., 12, 10051–10064, https://doi.org/10.5194/acp-12-10051-2012, 2012.

CIAO: CNR-IMAA Atmospheric Observatory, https://ciao.imaa.cnr.it, last access: 4 December 2023.

CIAO publications: https://ciao.imaa.cnr.it/publications/, last access: 10 December 2023.

Cubison, M. J., Ortega, A. M., Hayes, P. L., Farmer, D. K., Day, D., Lechner, M. J., Brune, W. H., Apel, E., Diskin, G. S., Fisher, J. A., Fuelberg, H. E., Hecobian, A., Knapp, D. J., Mikoviny, T., Riemer, D., Sachse, G. W., Sessions, W., Weber, R. J., Weinheimer, A. J., Wisthaler, A., and Jimenez, J. L.: Effects of aging on organic aerosol from open biomass burning smoke in aircraft and laboratory studies, Atmos. Chem. Phys., 11, 12049–12064, https://doi.org/10.5194/acp-11-12049-2011, 2011.

Deliverable 5.1: ACTRIS NF Labelling Plan, https://www.actris.eu/sites/default/files/Documents/ACTRISIMP/Deliverables/ACTRISIMP_WP5_D5.1_ACTRISNFLabellingPlan.pdf, last access: 24 November 2024.

De Rosa, B., Amato, F., Amodeo, A., D'Amico, G., Dema, C., Falconieri, A., Giunta, A., Gumà-Claramunt, P., Kampouri, A., Solomos, S., Mytilinaios, M., Papagiannopoulos, N., Summa, D., Veselovskii, I., and Mona, L.: Characterization of Extremely Fresh Biomass Burning Aerosol by Means of Lidar Observations, Remote Sens., 14, 4984, https://doi.org/10.3390/rs14194984, 2022.

Drinovec, L., Močnik, G., Zotter, P., Prévôt, A. S. H., Ruckstuhl, C., Coz, E., Rupakheti, M., Sciare, J., Müller, T., Wiedensohler, A., and Hansen, A. D. A.: The "dual-spot" Aethalometer: an improved measurement of aerosol black carbon with real-time loading compensation, Atmos. Meas. Tech., 8, 1965–1979, https://doi.org/10.5194/amt-8-1965-2015, 2015.

Dušan, J., Ďurčanská, D., and Bujdos, M.: The contribution of road traffic to particulate matter and metals in air pollution in the vicinity of an urban road, Transport and Environment, 50, 397–408, https://https://doi.org/10.1016/j.trd.2016.11.024, 2017

Esteve, A. R., Estelleìs, V., Utrillas, M. P., and Martiìnez-Lozano, J. A.: In-situ integrating nephelometer measurements of the scattering properties of atmospheric aerosols at an urban coastal site in western Mediterranean, Atmos. Environ., 47, 43–50, https://doi.org/10.1016/j.atmosenv.2011.11.043, 2012.

Fernandez, A. J., Sicard, M., Costa, M. J., Guerrero-Rascado, J. L., Gómez-Amo, J. L., Molero, F., Barragán, R., Basart, S., Bortoli, D., Bedoya-Velásquez, A. E., Utrillas, M. P., Salvador, P., Granados-Muñoz, M. J., Potes, M., Ortiz-Amezcua, P., Martínez-Lozano, J. A., Artíñano, B., Muñoz-Porcar, C., Salgado, R., Román, R., Rocadenbosch, F., Salgueiro, V., Benavent-Oltra, J. A., Rodríguez-Gómez, A., Alados-Arboledas, L., Comerón, A., and Pujadas, M.: Extreme, wintertime Saharan dust intrusion in the Iberian Peninsula: lidar monitoring and evaluation of dust forecast models during the February 2017 event, Atmos. Res., 228, 223–241, https://doi.org/10.1016/j.atmosres.2019.06.007, 2019.

Freudenthaler, V., Esselborn, M., Wiegner, M., Heese, B., Tesche, M., Ansmann, A., Müller, D., Althausen, D., Wirth, M., Fix, A., Ehret, G., Knippertz, P., Toledano, C., Gasteiger, J., Garhammer, M., and Seefeldner, M.: Depolarization ratio profiling at several wavelengths in pure Saharan dust during SAMUM 2006, Tellus B., 61, 165–179, https://doi.org/10.1111/j.1600-0889.2008.00396.x, 2009.

Fröhlich, R., Cubison, M. J., Slowik, J. G., Bukowiecki, N., Prévôt, A. S. H., Baltensperger, U., Schneider, J., Kimmel, J. R., Gonin, M., Rohner, U., Worsnop, D. R., and Jayne, J. T.: The ToF-ACSM: a portable aerosol chemical speciation monitor with TOFMS detection, Atmos. Meas. Tech., 6, 3225–3241, https://doi.org/10.5194/amt-6-3225-2013, 2013.

Gonçalves, C., Alves, C., Evtyugina, M., Mirante, F., Pio, C., Caseiro, A., Schmidl, C., Bauer, H., and Carvalho, F.: Characterisation of PM_{10} emissions from wood-stove combustion of com-

mon woods grown in Portugal, Atmos. Environ., 44, 4474–4480, https://doi.org/10.1016/j.atmosenv.2010.07.026, 2010.

Ilić, L., Jovanović, A., Kuzmanoski, M., Lazić, L., Madonna, F., Rosoldi, M., Mytilinaios, M., Marinou, E., and Ničković, S.: Mineralogy sensitive immersion freezing parameterization in DREAM, J. Geophys. Res.-Atmos., 127, e2021JD035093, https://doi.org/10.1029/2021JD035093, 2022.

IPCC: Aerosols and their impact on climate and human health. In Climate Change 2021: The Physical Science Basis, Contribution of Working Group I to the Sixth Assessment Report of the Intergovernmental Panel on Climate Change (IPCC), Cambridge University Press, https://doi.org/10.1017/9781009157896, 2021.

Kim, H. K., Choi, Y., and Ghim, Y. S.: Characterization of volatilization of filter-sampled $PM_{2.5}$ semi-volatile inorganic ions using a backup filter and denuders, Aerosol Air Qual. Res., 15, 814–820, https://doi.org/10.4209/aaqr.2014.09.0213, 2015.

Laj, P., Myhre, C. L., Riffault, V., Amiridis, V., Fuchs, H., Eleftheriadis, K., Petäjä, T., Salameh, T., Kivekäs, N., Juurola, E., Saponaro, G., Philippin, S., Cornacchia, C., Arboledas L. A., Baars, H., Claude, A., De Maziére, M., Dils, B., Dufresne, M., Enamgeliou, N., Favez. O., Fiebig, M., Haeffelin, M., Hermann, H., Höhler, K., Illmann, N., Kreuter, A., Ludewig, E., Marinou, E., Möhler, O., Mona, L., Murberg, L. E., Vicolae, D., Novelli, A., O'Connor, E., Ohneiser, K., Petracca Altieri, R. M. Picquet-Varrault, B., Van Pinxteren, D., Pospichal, B., Putaud, J-P., Reimann, S., Siomos, N., Stachlewska, I., Tillmann, R., Voudori, K. A., Wandinger, U., Wiedensohler, A., Apituley, A., Comerón, A., Gysel-Beer, M., Mihalopoulos N., Nikolova. N., Pietruczuk, A., Sauvage, S., Sciare, J., Skov, H., Svendby, T., Swietlicki, E., Tonev, D., Vaughan, G., Zdimal, V., Baltensperger, U., Doussin, J.-F., Kulmala, M., Pappalardo, G., Sundet, S. S., and Vana, M.: Aerosol, Clouds and Trace Gases Infrastructure (ACTRIS); The European Research Infrastructure Supporting Atmospheric Science, B. Am. Meteor. Soc., 105, E1098–E1136, https://doi.org/10.1175/BAMS-D-23-0064.1, 2024.

Laurita, T., Mona, L., De Rosa, B., Mytilinaios, M., Cardellicchio, F., Trippetta, S., Ripepi, E., and Volini, M.: CIAO main upgrade: building up an ACTRIS-compliant aerosol in situ laboratory, Version 1, National Research Council – Institute of Methodologies for Environmental Analysis [data set], https://doi.org/10.71763/2KZ1-X145, 2025.

Levin, Z., Ganor, E., and Gladstein, V.: The effects of desert particles coated with sulphate on rain formation in the Eastern Mediterranean, J. Appl. Meteorol., 35, 1511–1523, https://doi.org/10.1175/1520-0450(1996)035<1511:TEODPC>2.0.CO;2, 1996.

Levin, Z., Teller, A., Ganor, E. and Yin, Y.: On the interactions of mineral dust, sea-salt particles, and clouds: a measurement and modeling study from the Mediterranean Israeli Dust Experiment campaign, J. Geophys. Res., 110, D20202, https://doi.org/10.1029/2005JD005810, 2005.

Lopatin, A., Dubovik, O., Chaikovsky, A., Goloub, P., Lapyonok, T., Tanré, D., and Litvinov, P.: Enhancement of aerosol characterization using synergy of lidar and sun-photometer coincident observations: the GARRLiC algorithm, Atmos. Meas. Tech., 6, 2065–2088, https://doi.org/10.5194/amt-6-2065-2013, 2013.

Madonna, F., Amodeo, A., Cornacchia, C., D'Amico, G., Mona, L., Pandolfi, M., Pappalardo, G., and Cuomo, V.: Multichannel microwave radiometer and water vapour Raman lidar: comparisons and synergies, AITinforma – Rivista Italiana di telerilevamento, 35, 115–130, 2006.

Madonna, F., Amodeo, A., D'Amico, G., Mona, L., and Pappalardo, G.: Observation of non-spherical ultragiant aerosol using a microwave radar, Geophys. Res. Lett., 37, L21814, https://doi.org/10.1029/2010GL044999, 2010.

Madonna, F., Amodeo, A., Boselli, A., Cornacchia, C., Cuomo, V., D'Amico, G., Giunta, A., Mona, L., and Pappalardo, G.: CIAO: the CNR-IMAA advanced observatory for atmospheric research, Atmos. Meas. Tech., 4, 1191–1208, https://doi.org/10.5194/amt-4-1191-2011, 2011.

Madonna, F., Amato, F., Vande Hey, J., and Pappalardo, G.: Ceilometer aerosol profiling versus Raman lidar in the frame of the INTERACT campaign of ACTRIS, Atmos. Meas. Tech., 8, 2207–2223, https://doi.org/10.5194/amt-8-2207-2015, 2015.

Mahowald, N., Albani, S., Kok, J. F., Engelstaeder, S., Scanza, R., Ward, D. S., and Flanner, M. G.: The size distribution of desert dust aerosols and its impact on the Earth system, Aeolian Res., 15, 53–71, https://doi.org/10.1016/j.aeolia.2013.09.002, 2014.

Mărmureanu, L., Marin, C. A., Andrei, S., Antonescu, B., Ene, D., Boldeanu, M., Vasilescu, J., Viţelaru, C., Cadar, O., and Levei, E.: Orange Snow–A Saharan Dust Intrusion over Romania During Winter Conditions, Remote Sens., 11, 2466, https://doi.org/10.3390/rs11212466, 2019

Matthias, V., Balis, D., Bosenberg, J., Eixmann, R., Iarlori, M., Komguem, L., Mattis, I., Papayannis, A., Pappalardo, G., Perrone, M. R., and Wang, X.: Vertical aerosol distribution over Europe: Statistical analysis of Raman lidar data from 10 European Aerosol Research Lidar Network (EARLINET) stations, J. Geophys. Res.-Atmos., 109, D18201, https://doi.org/10.1029/2004JD004638, 2004.

Middlebrook, A. M., Bahreini, R., Jimenez, J. L., and Canagaratna, M. R.: Evaluation of composition-dependent collection efficiencies for the Aerodyne Aerosol Mass Spectrometer using field data, Aerosol Sci. Tech., 46, 258–271, https://doi.org/10.1080/02786826.2011.620041, 2012.

Molero, F., Pujadas, M., and Artinano, B.: Study of the Effect of Aerosol Vertical Profile on Microphysical Properties Using GRASP Code with Sun/Sky Photometer and Multiwavelength Lidar Measurements, Remote Sens., 12, 4072–4089, https://doi.org/10.3390/rs12244072, 2020.

Mona, L., Amodeo, A., Pandolfi, M., and Pappalardo, G.: Saharan dust intrusions in the Mediterranean area: three years of Raman lidar measurements, J. Geophys. Res., 111, D16203, https://doi.org/10.1029/2005JD006569, 2006.

Mona, L., Cornacchia, C., D'Amico, G., Di Girolamo, P., Pappalardo, G., Pisani, G., Summa, D., Wang, X., and Cuomo, V.: Characterization of the variability of the humidity and cloud fields as observed from a cluster of ground-based lidar systems, Q. J. Roy. Meteor. Soc., 133, 257–271, https://doi.org/10.1002/qj.160, 2007.

Mona, L., Pappalardo, G., Amodeo, A., D'Amico, G., Madonna, F., Boselli, A., Giunta, A., Russo, F., and Cuomo, V.: One year of CNR-IMAA multi-wavelength Raman lidar measurements in coincidence with CALIPSO overpasses: Level 1 products comparison, Atmos. Chem. Phys., 9, 7213–7228, https://doi.org/10.5194/acp-9-7213-2009, 2009.

Mona, L., Amodeo, A., D'Amico, G., Giunta, A., Madonna, F., and Pappalardo, G.: Multi-wavelength Raman lidar

observations of the Eyjafjallajökull volcanic cloud over Potenza, southern Italy, Atmos. Chem. Phys., 12, 2229–2244, https://doi.org/10.5194/acp-12-2229-2012, 2012.

Mona, L., Papagiannopoulos, N., Basart, S., Baldasano, J., Binietoglou, I., Cornacchia, C., and Pappalardo, G.: EARLINET dust observations vs. BSC-DREAM8b modeled profiles: 12-year-long systematic comparison at Potenza, Italy, Atmos. Chem. Phys., 14, 8781–8793, https://doi.org/10.5194/acp-14-8781-2014, 2014.

Mona, L., Amiridis, V., Cuevas, E., Gkikas, A., Trippetta, S., Vendenbussche, S., Benedetti, a., Dagsson-Waldhauserova, P., Formenti, P., Haefele, A., Kazadzis, S., Knippertz, P., Laurent, B., Madonna, F., Nickovic, S., Papagiannopoulos, N., Pappalardo, G., García-Pando, C. P., Popp, T., Rodríguez, S., Sealy, A., Sugimoto, N., Terradellas, E., Vimic, A. V., Weinzieri, B., and Basart, S.: Observing Mineral Dust in Northern Africa, the Middle East, and Europe: Current Capabilities and Challenges ahead for the Development of Dust Services, B. Am. Meteor. Soc., 104, E2223–E2264, https://doi.org/10.1175/BAMS-D-23-0005.1, 2023.

Mona, L., D'Amico, G., Ciamprone, S., Ripepi, E., Amato, F., and Dema, C., Gumà-Claramunt, P.: ACTRIS/EARLINET Level 3 2000–2019 Climatological Dataset Collection, ACTRIS ARES Data Centre, Version 1, National Research Council– Institute of Methodologies for Environmental Analysis [data set], https://doi.org/10.57837/cnr-imaa/ares/actrisearlinet/level3/climatological/2000_2019/pot, 2024.

Monteiro, A., Basart, S., Kazadzis, S., Votsis, A., Gkikas, A., Vandenbussche, S., Tobias, A., Gama, C., García-Pando, C. P., Terradellas, E., Notas, G., Middleton, N., Kushta, J., Amiridis, V., Lagouvardos, K., Kosmopoulos, P., Kotroni, V., Kanakidou, M., Mihalopoulos, N., Kalivitis, N., Dagsson-Waldhauserová, P., El-Askary, H., Sievers, K., Giannaros, T., Mona, L., Hirtl, M., Skomorowski, P., Virtanen, T.H., Christoudias, T., Di Mauro, B., Trippetta, S., Kutuzov, S., Meinander, O., and Nickovic, S.: Multi-sectoral impact assessment of an extreme African dust episode in the Eastern Mediterranean in March 2018, Sci. Total Environ., 843, 156861, https://doi.org/10.1016/j.scitotenv.2022.156861, 2022.

NASA Goddard Space Flight Center: AERONET-AErosol RObotic NETwork, NASA/GSFC, https://aeronet.gsfc.nasa.gov, last access: 15 November 2024.

Ng, N. L., Herndon, S. C., Trimborn, A., Canagaratna, M. R., Croteau, P. L., Onasch, T. B., Sueper, D., Worsnop, D. R., Zhang, Q., Sun, Y. L., and Jayne, J. T.: An aerosol chemical speciation monitor (ACSM) for routine monitoring of the composition and mass concentrations of ambient aerosol, Aerosol Sci. Tech., 45, 780–794, https://doi.org/10.1080/02786826.2011.560211, 2011.

Nicolae, D., Talianu, C., Vasilescu, J., Belegante, L., and Radu, C. M.: Characterization of fresh and aged biomass burning events using multiwavelength Raman lidar and mass spectrometry, J. Geophys. Res.-Atmos., 118, 2956–2965, https://doi.org/10.1002/jgrd.50324, 2013.

Nicolae, D., Vasilescu, J., Talianu, C., Binietoglou, I., Nicolae, V., Andrei, S., and Antonescu, B.: A neural network aerosol-typing algorithm based on lidar data, Atmos. Chem. Phys., 18, 14511–14537, https://doi.org/10.5194/acp-18-14511-2018, 2018.

Ohneiser, K., Ansmann, A., Chudnovsky, A., Engelmann, R., Ritter, C., Veselovskii, I., Baars, H., Gebauer, H., Griesche, H., Radenz, M., Hofer, J., Althausen, D., Dahlke, S., and Maturilli, M.: The unexpected smoke layer in the High Arctic winter stratosphere during MOSAiC 2019–2020 , Atmos. Chem. Phys., 21, 15783–15808, https://doi.org/10.5194/acp-21-15783-2021, 2021.

Pacifico, L. R., Pizzolante, A., Guarino, A., Iannone, A., Esposito, M., and Albanese, S.: Wildfire as a Source of Potentially Toxic Elements (PTSe) in Soil: A Case Study from Campania Region (Italy), Int. J. Environ. Res. Pub. He., 20, 4513, https://doi.org/10.3390/ijerph20054513, 2023.

Pakkanen, T. A., Loukkola, K., Korhonen, C. H., Aurela, M., Makela, T., Hillamo, R. E., Aarnio, P., Koskentalo, T., Kousa, A., and Maenhaut, W.: Sources and chemical composition of atmospheric fine and coarse particles in the Helsinki area, Atmos. Environ., 35, 5381–5391, http://hdl.handle.net/1854/LU-138499, 2001.

Papagiannopoulos, N., Mona, L., Amodeo, A., D'Amico, G., Gumà Claramunt, P., Pappalardo, G., Alados-Arboledas, L., Guerrero-Rascado, J. L., Amiridis, V., Kokkalis, P., Apituley, A., Baars, H., Schwarz, A., Wandinger, U., Binietoglou, I., Nicolae, D., Bortoli, D., Comerón, A., Rodríguez-Gómez, A., Sicard, M., Papayannis, A., and Wiegner, M.: An automatic observation-based aerosol typing method for EARLINET, Atmos. Chem. Phys., 18, 15879–15901, https://doi.org/10.5194/acp-18-15879-2018, 2018.

Pappalardo, G., Amodeo, A., Mona, L., Pandolfi, M., Pergola, N., and Cuomo, V.: Raman lidar observations of aerosol emitted during the 2002 Etna eruption, Geophys. Res. Lett., 31, L05120, https://doi.org/10.1029/2003GL019073, 2004a.

Pappalardo, G., Amodeo, A., Pandolfi, M., Wandinger, U., Ansmann, A., Bosenberg, J., Matthias, V., Amiridis, V., de Tomasi, F., Frioud, M., Iarlori, M., Komguem, L., Papayannis, A., Rocadenbosch, F., and Wang, X.: Aerosol lidar intercomparison in the framework of EARLINET, Part III. Raman lidar algorithm for aerosol extinction, backscatter and lidar ratio, Appl. Opt., 43, 5370–5385, https://doi.org/10.1364/AO.43.000977, 2004b.

Pappalardo, G., Mona, L., D'Amico, G., Wandinger, U., Adam, M., Amodeo, A., Ansmann, A., Apituley, A., Alados Arboledas, L., Balis, D., Boselli, A., Bravo-Aranda, J. A., Chaikovsky, A., Comeron, A., Cuesta, J., De Tomasi, F., Freudenthaler, V., Gausa, M., Giannakaki, E., Giehl, H., Giunta, A., Grigorov, I., Groß, S., Haeffelin, M., Hiebsch, A., Iarlori, M., Lange, D., Linné, H., Madonna, F., Mattis, I., Mamouri, R.-E., McAuliffe, M. A. P., Mitev, V., Molero, F., Navas-Guzman, F., Nicolae, D., Papayannis, A., Perrone, M. R., Pietras, C., Pietruczuk, A., Pisani, G., Preißler, J., Pujadas, M., Rizi, V., Ruth, A. A., Schmidt, J., Schnell, F., Seifert, P., Serikov, I., Sicard, M., Simeonov, V., Spinelli, N., Stebel, K., Tesche, M., Trickl, T., Wang, X., Wagner, F., Wiegner, M., and Wilson, K. M.: Four-dimensional distribution of the 2010 Eyjafjallajökull volcanic cloud over Europe observed by EARLINET, Atmos. Chem. Phys., 13, 4429–4450, https://doi.org/10.5194/acp-13-4429-2013, 2013.

PER-ACTRIS-IT Project: https://www.imaa.cnr.it/en/projects/38-attivita/progetti/713-per-actris-it, last access: 6 December 2023.

Perma Pure: MD-700 User Manual, https://www.permapure.com/wp-content/uploads/2014/06/MD-700-User-Manual.pdf, last access: 10 December 2023.

Perma Pure: Monotube Dryer 700 (MD-700), https://www.permapure.com/environmental-scientific/products/humidity-control-particle-aerosol-analysis/md-700-series-dryer-for-aerosol-analysis/, last access: 16 November 2024.

Peters, T. M. and Leith, D.: Concentration measurement and counting efficiency of the aerodynamic particle sizer 3321, J. Aerosol Sci., 34, 627–634, https://doi.org/10.1016/S0021-8502(03)00030-2, 2003.

Petzold, A., Ogren, J. A., Fiebig, M., Laj, P., Li, S.-M., Baltensperger, U., Holzer-Popp, T., Kinne, S., Pappalardo, G., Sugimoto, N., Wehrli, C., Wiedensohler, A., and Zhang, X.-Y.: Recommendations for reporting "black carbon" measurements, Atmos. Chem. Phys., 13, 8365–8379, https://doi.org/10.5194/acp-13-8365-2013, 2013.

Pio, C., Cerqueira, M., Harrison, R. M., Nunes, T., Mirante, F., Alves, C., Oliveira, C., Sanchez de la Campa, A., Artíñano, B., and Matos, M.: OC/EC ratio observations in Europe: Re-thinking the approach for apportionment between primary and secondary organic carbon, Atmos. Environ., 45, 6121–6132, https://doi.org/10.1016/j.atmosenv.2011.08.045, 2011.

Pöschl, U.: Atmospheric Aerosols: Composition, Transformation, Climate and Health Effects, Angew. Chem. Int. Edit., 44, 7520–7540, https://doi.org/10.1002/anie.200501122, 2005.

Quattro Esse: http://www.quattro-esse.it/Home.html, last access: 24 November 2024.

Regione Basilicata: RSdi – Territorial Information System, http://rsdi.regione.basilicata.it, last access: 28 November 2023.

Rajšić, S., Mijić, Z., Tasić, M., Radenković, M., and Joksić, J.: Evaluation of the levels and sources of trace elements in urban particulate matter, Environ. Chem. Lett., 6, 95–100, https://doi.org/10.1007/s10311-007-0115-0, 2008.

Redemann, J. and Gao, L.: A machine learning paradigm for necessary observations to reduce uncertainties in aerosol climate forcing, Nat. Commun., 15, 8343, https://doi.org/10.1038/s41467-024-08343-1, 2024.

Ren-Jian, Z., Kin-Fai, H., and Zhen-Xing, S.: The Role of Aerosol in Climate Change, the Environment, and Human Health, Atmospheric and Oceanic Science Letters, 5, 156–161, https://doi.org/10.1080/16742834.2012.11446983, 2012.

Rodriguez-Navarro, C., di Lorenzo, F., and Elert, K.: Mineralogy and physicochemical features of Saharan dust wet deposited in the Iberian Peninsula during an extreme red rain event, Atmos. Chem. Phys., 18, 10089–10122, https://doi.org/10.5194/acp-18-10089-2018, 2018.

Rosoldi, M., Coppa, G., Merlone, A., Musacchio, C., and Madonna, F.: Intercomparison of Vaisala RS92 and RS41 Radiosonde Temperature Sensors under Controlled Laboratory Conditions, Atmosphere, 13, 773, https://doi.org/10.3390/atmos13050773, 2022.

Sandradewi, J., Prévôt, A. S. H., Szidat, S., Perron, N., Alfarra, M., Lanz, V. A., Weingartner, E., and Baltensperger, U.: Using Aerosol Light Absorption Measurements for the Quantitative Determination of Wood Burning and Traffic Emission Contributions to Particulate Matter, Environ. Sci. Technol., 42, 3316–3323, https://doi.org/10.1021/es702253m, 2008.

Sawamura, P., Vernier, J. P., Barnes, J. E., Berkoff, T. A., Welton, E. J., Alados-Arboledas, L., Navas-Guzmán, F., Pappalardo, G., and Madonna, F.: Stratospheric AOD after the 2011 eruption of Nabro volcano measured by lidar over the Northern Hemisphere, Environ. Res. Lett., 7, 031001, https://doi.org/10.1088/1748-9326/7/3/034013, 2012.

Schmid, O., Karg. E., Hagen, D. E., Whitefield, P. D., and Ferron, G. A.: On the effective density of non-spherical particles as derived from combined measurements of aerodynamic and mobility equivalent size, J. Aerosol Sci., 38, 431–443, https://doi.org/10.1016/j.jaerosci.2007.01.002, 2007.

Schmidl, C., Marr, I. L., Caseiro, A., Kotianovaì, P., Berner, A., Bauer, H., Kasper-Giebl, A., and Puxbaum, H.: Chemical characterization of fine particle emissions from wood stove combustion of common woods growing in mid-European Alpine regions, Atmos. Environ., 42, 126–141, https://doi.org/10.1016/j.atmosenv.2007.09.028, 2008.

Sirignano, C., Riccio, A., Chianese, E., Ni, H., Zenker, K., D'Onofrio, A., Meijer, H. A. J., and Dusek, U.: High Contribution of Biomass Combustion to $PM_{2.5}$ in the City Centre of Naples (Italy), Atmosphere, 10, 451, https://doi.org/10.3390/atmos10080451, 2019.

Sokolik, I. N. and Toon, O. B.: Direct radiative forcing by anthropogenic airborne mineral aerosols, Nature, 381, 681–683, https://doi.org/10.1038/381681a0, 1996.

Soupiona, O., Papayannis, A., Kokkalis, P., Foskinis, R., Sánchez Hernández, G., Ortiz-Amezcua, P., Mylonaki, M., Papanikolaou, C.-A., Papagiannopoulos, N., Samaras, S., Groß, S., Mamouri, R.-E., Alados-Arboledas, L., Amodeo, A., and Psiloglou, B.: EARLINET observations of Saharan dust intrusions over the northern Mediterranean region (2014–2017): properties and impact on radiative forcing, Atmos. Chem. Phys., 20, 15147–15166, https://doi.org/10.5194/acp-20-15147-2020, 2020.

TSI company: https://tsi.com/home/ last access: 15 November 2024.

Veselovskii, I., Dubovik, O., Kolgotin, A., Korenskiy, M., Whiteman, D. N., Allakhverdiev, K., and Huseyinoglu, F.: Linear estimation of particle bulk parameters from multi-wavelength lidar measurements, Atmos. Meas. Tech., 5, 1135–1145, https://doi.org/10.5194/amt-5-1135-2012, 2012.

Viana, M., Chi, X., Maenhaut, W., Cafmeyer, J., Querol, X., Alastuey, A., Mikuška, P., and Večeřa, Z.: Influence of sampling artefacts on measured PM, OC, and EC Levels in carbonaceous aerosols in an urban area, Aerosol Sci. Tech., 40, 107–117, https://doi.org/10.1080/02786820500484388, 2006.

Villani, M. G., Mona, L., Maurizi, A., Pappalardo, G., Tiesi, A., Pandolfi, M., D'Isidoro, M., Cuomo, V., and Tampieri, F.: Transport of volcanic aerosol in the troposphere: the case study of the 2002 Etna plume, J. Geophys. Res., 111, D21102, https://doi.org/10.1029/2006JD007126, 2006.

Vratolis, S., Fetfatzis, P., Argyrouli, A., Soupiona, O., Mylonaki, M., Maroufidis, J., Kalogridis, A. C., Manousakas, M., Bezantakos, S., Binietoglou, I., Labzovskii, L. D., Solomos, S., Papayannis, A., Močnik, G., O'Connor, E., Müllerf, D., Tzanisl, C. G., and Eleftheriadis, K.: Comparison and complementary use of in situ and remote sensing aerosol measurements in the Athens Metropolitan Area, Atmos. Environ., 228, 117439, https://doi.org/10.1016/j.atmosenv.2020.117439, 2020.

Wiedensohler, A., Birmili, W., Putaud, J. P., and Ogren, J.: Recommendations for Aerosol Sampling, in: Aerosol Science: Technology and Applications, First Edition, edited by: Colbeck, I. and Lazaridis, M., John Wiley & Sons, Ltd., 45–59, https://doi.org/10.1002/9781118682555.ch3, 2014.

WMO/GAW: Aerosol Measurement Procedures, Guidelines and Recommendations 2nd Edition, No. 227, Zenodo, https://doi.org/10.5281/zenodo.11145571, 2016.

Zhi, M., Zhang, X., Zhang, K., Ussher, S. J., Lv, W., Li, J., Gao, J., Luo, Y., and Meng, F.: The characteristics of atmospheric particles and metal elements during winter in Beijing: Size distribution, source analysis, and environmental risk assessment, Ecotox. Environ. Safe, 211, 111937, https://doi.org/10.1016/j.ecoenv.2021.111937, 2021.

Zhou, C. W., Huang, H., and Cao, J. J.: Summary of basic characteristics of atmospheric aerosol carbonaceous, Environ. Pollut. Control, 28, 270–274, 2006.

Zhao, Q., Huob, J., Yanga, X., Fub, Q., Duanb, Y., Liua, Y., Linb, Y., and Zhang, Q.: Chemical characterization and source identification of submicron aerosols from a year-long real-time observation at a rural site of Shanghai using an Aerosol Chemical Speciation Monitor, Atmos. Res., 246, 105154, https://doi.org/10.1016/j.atmosres.2020.105154, 2020.